

LA-UR-19-20146 (Accepted Manuscript)

## Evaluation of the Prompt Fission Gamma Properties for Neutron Induced Fission of $^{235}\text{U}$ , $^{238}\text{U}$ and $^{239}\text{Pu}$

Stetcu, Ionel  
Chadwick, Mark Benjamin  
Kawano, Toshihiko  
Talou, Patrick  
Capote, Roberto  
Trkov, Andrej

Provided by the author(s) and the Los Alamos National Laboratory (2020-02-13).

**To be published in:** Nuclear Data Sheets

**DOI to publisher's version:** 10.1016/j.nds.2019.12.007

**Permalink to record:** <http://permalink.lanl.gov/object/view?what=info:lanl-repo/lareport/LA-UR-19-20146>

**Disclaimer:**

Los Alamos National Laboratory, an affirmative action/equal opportunity employer, is operated by Triad National Security, LLC for the National Nuclear Security Administration of U.S. Department of Energy under contract 89233218CNA000001. By approving this article, the publisher recognizes that the U.S. Government retains nonexclusive, royalty-free license to publish or reproduce the published form of this contribution, or to allow others to do so, for U.S. Government purposes. Los Alamos National Laboratory requests that the publisher identify this article as work performed under the auspices of the U.S. Department of Energy. Los Alamos National Laboratory strongly supports academic freedom and a researcher's right to publish; as an institution, however, the Laboratory does not endorse the viewpoint of a publication or guarantee its technical correctness.

# Evaluation of the Prompt Fission Gamma Properties for Neutron Induced Fission of $^{235,238}\text{U}$ and $^{239}\text{Pu}$

I. Stetcu,<sup>1,\*</sup> M.B. Chadwick,<sup>1</sup> T. Kawano,<sup>1</sup> P. Talou,<sup>1</sup> R. Capote,<sup>2</sup> and A. Trkov<sup>2</sup>

<sup>1</sup>*Los Alamos National Laboratory, Los Alamos, NM 87545, USA*

<sup>2</sup>*International Atomic Energy Agency, Vienna-A-1400, PO Box 100, Austria*

(Received 2 April 2019; revised received 19 July and 15 August 2019; accepted 17 August 2019)

We present details of the prompt fission gamma property evaluations included in the released ENDF/B-VIII.0 files. The average prompt gamma multiplicity, the average prompt gamma spectrum, the average total prompt gamma energy released and the prompt gamma multiplicity distributions, included in the ENDF/B-VIII.0 files, are presented for  $^{235}\text{U}(n,f)$ ,  $^{238}\text{U}(n,f)$ , and  $^{239}\text{Pu}(n,f)$  reactions, as a function of incident neutron energy up to 30 MeV. The evaluation is based on available experimental data and model calculations. Notable data include recent measurements by experimental groups at Los Alamos and Lawrence Livermore National Laboratories, at Geel and Budapest, at CEA labs, as well as seminal historical gamma production measurements by Drake at Los Alamos.

## CONTENTS

I. INTRODUCTION	1
II. THEORETICAL MODELS	2
III. PFG EVALUATIONS	3
A. The $^{235}\text{U}(n,f)$ Reaction	4
1. Average PFGS	4
2. Average PFG Multiplicity and the Multiplicity Probability Distribution	6
3. Average Total PFG Energy	9
B. The $^{238}\text{U}(n,f)$ Reaction	9
C. The $^{239}\text{Pu}(n,f)$ Reaction	13
IV. CONCLUSIONS AND OUTLOOK	15
Acknowledgements	17
References	17

## I. INTRODUCTION

Properties of prompt fission gammas (PFG) have been measured in recent years for a variety of neutron-induced and spontaneous fission reactions, based on data taken at Los Alamos, Geel, Budapest and CEA. For neutron-induced reactions, these experiments have concentrated

on measuring prompt fission gamma spectra (PFGS), average PFG multiplicities and average photon energies for a limited number of incident neutron energies, with an emphasis on thermal neutrons. This is the main reason that for the evaluation of quantities like the average prompt gamma-ray multiplicity or multiplicity probability distribution as a function of incident neutron energies, we had to rely on some more inclusive data on total gamma production and on simulations. Understandably, the same amount of data is not available for all three reactions considered here, with much less information available for  $^{238}\text{U}(n,f)$ , a threshold fissioner, than for  $^{235}\text{U}(n,f)$  or  $^{239}\text{Pu}(n,f)$ . For this reason, the evaluation of the properties of prompt fission gamma-rays produced in the  $^{238}\text{U}(n,f)$  was inferred by using information extracted from the  $^{235}\text{U}(n,f)$  reaction. As PFG could become relevant for a suite of applications, experiments that constrain their properties, especially in the fast incident neutron energy range, would be extremely useful.

The current ENDF/B-VIII.0 evaluation [1] of the PFG properties represents a significant improvement over the previous releases. First, in ENDF/B-VII.1 [2], the PFG data were represented explicitly up to 1.09 MeV for  $^{235}\text{U}$  and  $^{239}\text{Pu}$ , with all channels lumped together into a production gamma-ray format above 1.09 MeV incident neutron energy. In the current evaluation, all open channels are represented explicitly up to 20–30 MeV incident neutron energy. This breakdown on different channels will allow in the future, as an option, the replacement of the evaluated fission data by event generators, like fission event generators CGMF [3] or FREYA [4] currently embedded in MCNP<sup>©</sup> [5], which provide correlations that are not or cannot be embedded in the evaluation files

---

\* Corresponding author: stetcu@lanl.gov

[6]. Second, newly available data on average PFG multiplicity and spectra have been used to inform the evaluation. In particular, the experimental results for  $^{235}\text{U}$  and  $^{239}\text{Pu}$  were incorporated into the evaluations of both the PFG spectra and average multiplicity. Finally, a new format has been introduced in ENDF file 6 for fission data, which allows representation of both neutron and gamma multiplicity probabilities, with an option to include the multiplicity-dependent spectra. In the current ENDF-B/VIII.0 evaluation, we only provide the multiplicity probability distributions, for reasons that will be extensively explained below. However, it is very likely that multiplicity-dependent spectra will be included in the next revision of the evaluation files.

Evaluations of physical observables should be a proper combination, in a Bayesian sense [7], of experimental measurements and model calculations. Much lower experimental uncertainties give a greater weight to experimental results, but models allow for extrapolations to regions where no data exist or are discrepant. But guidance from experiment is not always adequate to evaluate all the properties of interest. Hence, in some cases, and in particular for PFG multiplicity probability distributions,  $P(\nu_\gamma)$ , we have used simulations obtained with the code CGMF (Cascade Gamma-Ray Multiplicity for Fission) [3] developed in the Nuclear Data group at Los Alamos. In Sec. II, we present the main assumptions and features of the code, as well as other models used to compare against the current evaluation.

The amount of experimental data available for each reaction can vary significantly, and thus the degree to which adjustments to the simulation data are necessary. In section III, we present for each reaction the specific details of the evaluation of different observables. Finally, conclusions and an outlook are presented in Sec. IV.

## II. THEORETICAL MODELS

CGMF was the main theoretical model tool used in the PFG evaluations. In CGMF, the fission fragments (FFs) are assumed to be compound nuclei whose de-excitation towards a low-lying state (either ground or isomeric state) is modeled via neutron and gamma emissions, treated within the statistical Hauser-Feshbach formalism. The de-excitation of the FFs can be run in both deterministic and Monte Carlo modes, depending on the type of information one needs. Thus, if the goal is the PFG spectra at high outgoing gamma-ray energies, the deterministic mode is more efficient, as it includes rare events that cannot be easily sampled in a Monte Carlo approach. However, other observables, such as neutron or gamma multiplicity probabilities, or correlations between the emitted particles, can be only obtained in a Monte Carlo framework, where neutron and gamma emission probabilities are sampled in competition. Other implicit assumptions are that no neutrons are emitted at neck rupture or during the evolution from saddle to scission (so-called scis-

sion neutrons for which experimental evidence is scarce), and that all neutrons (and consequently gammas) are emitted from fully accelerated FFs. Finally, only binary fission events are considered.

Several ingredients (optical model, gamma-ray strength functions, mass, charge and total kinetic energy, usually abbreviated TKE, yields, *etc.*) are necessary in order to perform CGMF simulations. These are directly taken from or fitted to experimental data or inferred systematics. While we do not go into great details here in the implementation of the incident neutron energy dependence  $E_n$  in CGMF, we mention that the FF mass yields are constructed as a superposition of five Gaussians, with centroids and widths that depend on  $E_n$ . The charge distribution is obtained using Wahl systematics [8] and the parity is taken equiprobable, as discussed in our earlier papers that are restricted to spontaneous and neutron-induced fission reactions by thermal neutrons. We assume that for each fragmentation the TKE distribution is a Gaussian, with a  $E_n$ -independent width given by available data or systematics, and the average of mass that has the same shape of  $\langle \text{TKE} \rangle (A_{\text{FF}}, E_n)$  as for thermal neutrons, but scaled so that the average  $\langle \text{TKE} \rangle$  for the reaction decreases linearly with  $E_n$ , as observed experimentally below second-chance fission. For the emerging FFs, the spin probability distribution is taken simply as

$$P(J_{\text{FF}}) \propto (2J_{\text{FF}} + 1) \exp \left[ -\frac{J_{\text{FF}}(J_{\text{FF}} + 1)}{2B^2} \right], \quad (1)$$

where  $B$  is the spin cutoff parameter that depends on the mass, charge, and available excitation energy in the fission fragment. We take the cutoff parameter directly proportional to a global parameter  $\alpha$  that parameterizes the dependence on  $E_n$ . In our approach,  $\alpha(E_n)$  is adjusted to fine tune not only the average neutron multiplicity as a function of incident energy for  $E_n$  up to the second-chance fission threshold, but also measured gamma observables at thermal incident neutron energy for  $^{235}\text{U}$  and  $^{239}\text{Pu}$ . We use simple linear extrapolations to extend the energy dependence beyond the threshold for first chance fission. Such a simple extension, combined with using other parameters fixed at or close to stability (level densities, optical model, *etc.*), is subject to systematic errors that have not yet been thoroughly investigated.

The incident neutron energy considered in the evaluations varies from thermal to 20 or 30 MeV. In this interval, it is energetically possible that one or more neutrons be emitted before fission. Hence, we model the multi-chance fission by simulating the emission of neutrons in the parent fissioning system. When simulating the emission of the first neutron, if the incident neutron energy is large enough (above about 10 MeV), we also consider pre-equilibrium emission. The number of neutrons emitted before fission is sampled according to the multi-chance fission probabilities, obtained from double-hump fission barrier penetrability calculations, with parameters cho-

sen to follow the ENDF evaluation as closely as possible. Further details of the method are presented in previous publications [9–12].

In addition to CGMF simulations, we have used for comparison purposes only, the parameterization introduced by Oberstedt *et al.* [13, 14], even though this method is limited and subject to inconsistencies, as noted below. The explicit assumption in this approach is that the average gamma-ray multiplicity is proportional to the average number of neutrons emitted from the fission fragments. The basis of this work is an older measurement for  $^{252}\text{Cf}(\text{sf})$  by Nifenecker *et al.* [15] that found that the total PFG energy and the average PFG multiplicity are positively correlated with the average number of neutrons emitted from the FFs. The average PFG total energy released (in units of MeV) and the average PFG multiplicity is, thus, parameterized as

$$\langle E_{\gamma}^{\text{tot}} \rangle(E_n, Z, A) = (a_0 + a_1 \times Z^2 A^{1/2}) \langle \nu_n \rangle + 4, \quad (2)$$

$$\langle \nu_{\gamma} \rangle(E_n, Z, A) = (c_0 + c_1 \times Z^{5/3} A^{-1/2}) \langle \nu_n \rangle, \quad (3)$$

where  $\langle \nu_n \rangle$  is the average neutron multiplicity emitted from the fission fragments for fission induced by a neutron with incident energy  $E_n$ , with  $Z$  and  $A$  the charge and mass numbers of the fissioning system. The dependence on  $E_n$  is implicit, via the average neutron multiplicity  $\langle \nu_n \rangle$  emitted from the fission fragments. Note that in deriving Eq. (3) from Eq. (2), the authors assume that the average photon energy is independent of  $E_n$ ,  $\langle \varepsilon_{\gamma} \rangle = b_0 + b_1 \times Z^{1/3} A^{-1}$ . However, when the parameterizations (2) and (3) are used, the average gamma-ray energy, calculated as a ratio of average total PFG energy and average multiplicity ( $\langle \varepsilon_{\gamma} \rangle = \langle E_{\gamma}^{\text{tot}} \rangle / \langle \nu_{\gamma} \rangle$ ), presents a fairly strong dependence on the incident neutron energy, thus is inconsistent with the initial assumption. The parameters  $a_0$ ,  $a_1$ ,  $b_0$ ,  $b_1$ ,  $c_0$  and  $c_1$  are fitted to reproduce available measured data on several isotopes, with the error bars in this approach determined by the fit uncertainties. Above the threshold for multi-chance fission, the pre-fission neutrons are not included in  $\langle \nu_n \rangle$ .

Other more recent experiments [16–19], have not been able to reproduce the same strong positive correlation between the average neutrons emitted from FFs and the average total gamma-ray energy suggested by Ref. [15]. Hence, the model has its limitations.

For the  $^{238}\text{U}(\text{n},\text{f})$  reaction, we have also used theoretical results provided by A. Tudora [20], obtained using the point-by-point model [21], which is an extension of the Los Alamos prompt fission neutron model [22].

### III. PFG EVALUATIONS

Although there are slight differences from one reaction to another in the evaluation procedure, dictated mainly

by the available experimental data for each isotope, in all cases similar guidelines are observed. At thermal incident energy, we evaluate the average gamma multiplicity and PFGS from the available experimental data, with the exception of  $^{238}\text{U}$ , which is a threshold fissioner. In order to obtain PFG properties for thermal incident neutrons on  $^{238}\text{U}$  targets, we rescale the  $^{235}\text{U}(\text{n},\text{f})$  results, as will be discussed below. We further assume that the average PFGS is independent of the incident neutron energy. This assumption is supported by data and CGMF calculations, which show little variation of the PFGS with the incident neutron energy. Above thermal incident neutron energies, we use the measured total gamma production data to determine the average PFG multiplicity as a function of incident energy by subtracting the contribution of the other gamma producing channels, assuming that they can be properly accounted for by theoretical models. For all reactions, we provide (as a function of incident neutron energy) evaluations for the average PFG multiplicity, PFG energy spectra, and multiplicity-dependent gamma emission probability distributions.

In CGMF calculations, the average PFGS depends fairly weakly on the incident neutron energy. This weak dependence is illustrated in Fig. 1, where the average gamma-ray energy is plotted as a function of incident neutron energy. Equality in average gamma-ray energies for PFGS at different incident neutron energies does not guarantee identical spectra, but it is a good indication that these PFGS will be close to each other. While other moments should also be considered, we show later in the paper when we compare against the total gamma production spectra that our assumption is reasonable. At 20 MeV incident energy,  $\langle \varepsilon_{\gamma} \rangle$  is only 7% larger than the thermal value. This result is in agreement with measured spectra at different incident energies [23], but in contrast with Ref. [13, 14], where the authors predict a rather strong dependence on the incident energies. As discussed above, however, in this approach there is some inconsistency between the initial assumptions and the final results. Note that in CGMF calculations, the average gamma-ray energy exhibits various plateaux, with increases at the threshold for multi-chance fission. If the first increase is rather sharp at the threshold for second-chance fission, a softer slope is observed from 11 to 15 MeV incident neutron energy, as the onset of pre-equilibrium emission of pre-fission neutrons overlaps with the threshold for third-chance fission. Furthermore, while available data for the  $^{238}\text{U}(\text{n},\text{f})$  reaction also show little energy dependence below 6 MeV incident neutron energy (see Sec. III B), other experimental data paint a different picture at 15 MeV (see Fig. 6 in Ref. [24]). As some applications could be impacted, the dependence of the average gamma-ray energy with respect to the incident neutron energy should be constrained experimentally and included in future evaluations.

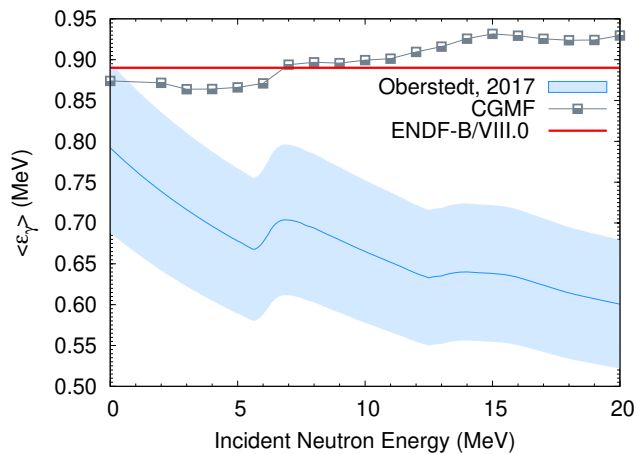


FIG. 1. (Color online) Average gamma-ray energy as a function of incident neutron energy, for the  $^{235}\text{U}(n,f)$  reaction. For this figure, we have used 100 keV threshold for the CGMF calculations. The shaded area shows the Oberstedt evaluation [14].

### A. The $^{235}\text{U}(n,f)$ Reaction

The PFG evaluations for the  $^{235}\text{U}(n,f)$  reaction are mainly based on direct and indirect experimental data, with theoretical input from CGMF for PFGS and  $P(\nu_\gamma)$ . Data are scarce for incident neutrons in the fast region, so that the main drivers for the evaluation above thermal neutron energies are measurements of the total gamma production [25–29], not only for  $^{235}\text{U}(n,f)$ , but also for the other two reactions considered in this evaluation. In previous evaluations, only data on the total gamma production were available [30], reflected by a lumped total gamma channel included in the evaluated data file above 1.09 MeV incident neutron energy. In contrast, in ENDF/B-VIII.0 all open channels producing gamma-rays have been explicitly given. In Table I we present a summary of the PFG properties in the ENDF/B-VIII.0 evaluation for neutron-induced fission with thermal neutrons in comparison with existing evaluations, and selected experimental data. The significant difference between the latest library and ENDF/B-VII.1 is due to the fact that previous evaluations at thermal incident neutron energies have been based on the Verbinski *et al.* measurement, while we have chosen to base our work on the most recent experiment by Oberstedt *et al.* The two measurements differ in two important ways: (i) the low-energy detection threshold (140 keV for Verbinski, 100 keV for Oberstedt), and (ii) more gamma-rays are observed by Oberstedt *et al.* between 140 and 300 keV outgoing gamma-ray energies. To the extent of our knowledge, there is no obvious reason for discrepancy between the two measurements. As a result of our choice to rely on the Oberstedt *et al.* data, the two evaluations are quite different at thermal incident neutron energy. When the threshold for gamma-ray detection in Table I is increased, the relative disagree-

TABLE I. Evaluation of prompt fission gamma-ray properties for  $^{235}\text{U}(n_{\text{th}},f)$ : comparison between the current evaluations, experimental data and CGMF calculations. We present the average gamma multiplicity,  $\langle \nu_\gamma \rangle$ , the average gamma-ray energy,  $\langle \varepsilon_\gamma \rangle$ , and the total prompt gamma energy released,  $\langle E_\gamma^{\text{tot}} \rangle$ . All energies are in MeV. Similar time coincidence windows have been employed in all experiments included in this compilation, ranging from 6 to 10 ns.

	$E_{\text{thresh}}$	$\langle \nu_\gamma \rangle$	$\langle \varepsilon_\gamma \rangle$	$\langle E_\gamma^{\text{tot}} \rangle$
ENDF/B-VIII.0	0	8.58	0.85	7.28
ENDF/B-VII.1		7.04	0.94	6.60
JEFF-3.3		8.74	0.81	7.05
JENDL 4		7.43	0.94	6.96
CGMF		7.94	0.78	6.20
ENDF/B-VIII.0	0.10	8.19	0.89	7.25
ENDF/B-VII.1	0.10	6.87	0.96	6.59
Pleasanton [31]	0.09	6.51(30)	0.99(7)	6.43(30)
Oberstedt 2013 [32, 33]	0.10	8.19(11)	0.84(2)	6.92(9)
Oberstedt 2017 [34]	0.10	7.22	0.87	6.27
CGMF	0.10	7.01	0.87	6.15
ENDF/B-VIII.0	0.14	7.78	0.93	7.21
ENDF/B-VII.1	0.14	6.72	0.98	6.57
Verbinski [35]	0.14	6.7(3)	0.97(5)	6.51(30)
Oberstedt 2017 [33]	0.14	7.01(18)	0.89(4)	6.24(20)
CGMF	0.14	6.68	0.91	6.10
Chyzh [36]	0.15	7.35		8.35
Peelle [37]	0.15	7.45(35)	0.99(7)	7.18(26)
ENDF/B-VIII.0	0.40	5.47	1.21	6.60
ENDF/B-VII.1	0.40	5.30	1.17	6.17
Jandel [38]	0.40	4.92	1.20	5.89
CGMF	0.40	4.87	1.19	5.78
Valentine [39, 40]				6.53(3)

ment between the evaluations decreases for the average gamma-ray multiplicity and average gamma-ray energy.

#### 1. Average PFGS

At thermal neutron incident energies, quite a few measurements of the PFGS exist [32, 35–38, 41]. In particular, the latest measurements at the KFKI reactor in Budapest [32] have used high-resolution LaBr<sub>3</sub> detectors and provide an excellent separation of low-energy peaks produced by decays within low-lying discrete states in fission fragments. Such high accuracy experiments provide excellent testing ground for theoretical models, and in particular CGMF, which was the main theoretical model used in this evaluation. The data by Oberstedt *et al.* were preferred for the evaluation, as the detectors had a lower energy threshold that revealed a significant number of gamma-rays emitted at low energies than previously measured in other experiments. We note that the original data published in Ref. [32] were recently reanalyzed and a calibration error was discovered [33]. This error has not changed the results for the average PFG multiplicity reported in Ref. [32], but has shifted by a few keV the location of the peaks. As a consequence of this correction,

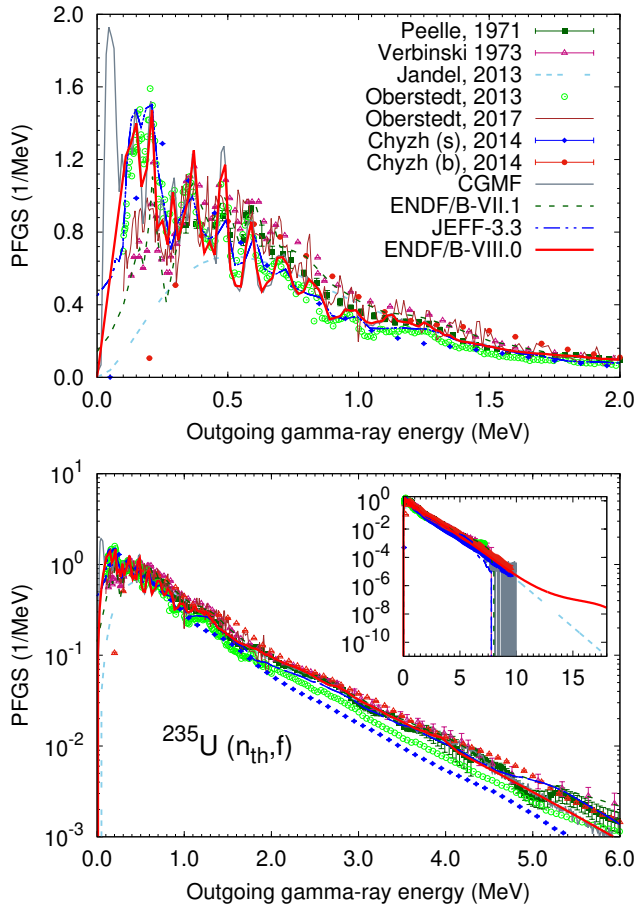


FIG. 2. (Color online) Average prompt fission gamma spectrum for thermal incident neutron energy. The evaluations are normalized to one, but the experimental data are rescaled so that within the range of measurement for each dataset reproduces the normalization of ENDF/B-VIII.0 within the same interval. In the upper panel, we present the data at low energies (below 2 MeV) on a linear scale, while in the lower panel we show the evaluation and data up to 5 MeV on a lin-log scale. In the insert, we show the spectrum up to 20 MeV outgoing gamma-ray energy. Data was taken from Ref. [32, 34, 35, 37, 41]. The Chyzh *et al.* data were unfolded by two methods: Bayesian (b) and Singular Value Decomposition (s), and our ENDF/B-VIII.0 evaluation lies between them. The Jandel data were constructed from the parameterization given in Ref. [38].

the CGMF PFGS is in better agreement with the corrected data set at low outgoing gamma-ray energies that it was with the originally reported measurement, as illustrated in the upper panel of Fig. 2.

An additional measurement was performed by the same group and the results provided to us [33], for outgoing energies up to 2 MeV and extrapolated above 2 MeV. While the new measurement suffers from lack of statistics, it also shows a stark discrepancy with the previous 2013 measurement below 300 keV, which is hard to quantify since no uncertainties were provided. As shown in Fig. 2, the

new data lie closer to the Verbinski result below 300 keV. However, because the new measurement was not peer-reviewed at the time of the evaluation, we have decided to use CGMF calculations in the evaluation of the PFGS, from 0.1 to 6 MeV, since they agree well with the corrected 2013 data. In addition, as shown in Fig. 2, reasonable agreement is obtained with previous measurements of the PFGS of Peelle [37] and Verbinski [35] between 2 and 5 MeV. Above 6 MeV, we have combined CGMF calculations in semi-deterministic mode (the gamma-ray spectra are calculated deterministically from fission fragments sampled from the complete  $Y(Z_{FF}, A_{FF}, TKE, U, J, \pi)$  yield distribution in charge, mass, TKE, excitation energy, spin, and parity) with the latest data by Nishio *et al.* [42], obtained with an experimental setup that targets high-energy gamma-rays. Note that in Fig. 2, the evaluated spectra are normalized to one, while the experimental data were rescaled so that within the measured range of outgoing gamma-ray energies, we obtain the same normalization as in ENDF/B-VIII.0. Below 100 keV, the CGMF calculations are plagued by spurious effects arising from the discrete representation of the continuum in Hauser-Feshbach calculations, and cannot be used for the evaluation. The evaluated spectrum increases linearly from 0 to the CGMF value at 100 keV.

The ENDF/B-VIII.0 evaluation is in reasonable agreement with the data published by the Livermore-Los Alamos collaboration [41]. The experimental data have been unfolded using two methods, Bayesian and Singular Value Decomposition (SVD), and the evaluation is in between the two measurements, which are not consistent within the quoted uncertainties. In addition, we compare with the parameterized model introduced by Jandel *et al.* [38]. Because the model does not describe the low-energy region well, we have used a range from 0.4 MeV to 20 MeV to renormalize the PFGS. Excellent agreement is observed from 0.4 MeV up to about 7 MeV. At higher energies, the model is not expected to correctly simulate the PFGS, as the physics of the giant dipole resonance is not included.

It can be immediately seen from Table I that the evaluated average PFGS in ENDF/B-VIII.0 is softer than in ENDF/B-VII.1, where the basis for the evaluation was the measurement by Verbinski [35]. From 2 to about 4.8 MeV outgoing gamma-ray energies, the new evaluation closely follows the Verbinski spectrum. However, around 4.8 MeV, the Verbinski spectrum becomes softer, and while such a change is expected, based on recent experiments by Nishio's group [42], this change, determined by the giant dipole resonance in FFs, should occur at higher outgoing energies. The spectrum measured by Oberstedt tends to be softer than both Peelle and Verbinski measured spectra.

At higher incident neutron energies, no experimental data are available for the PFGS. Hence, in order to assess the quality of the evaluated average PFGS, we use the

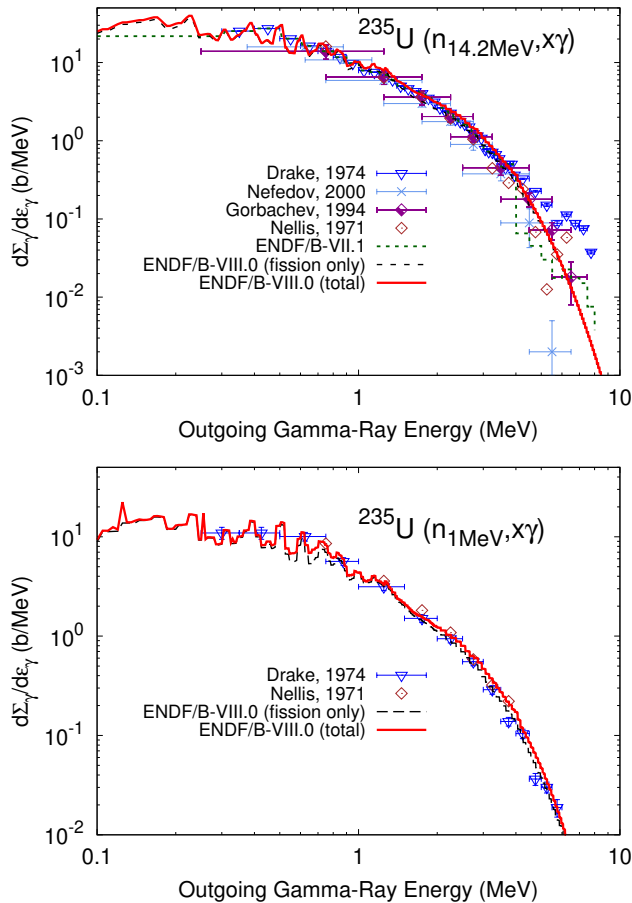


FIG. 3. (Color online) Differential total gamma production cross section as a function of outgoing gamma-ray energy for 1 and 14.2 incident neutrons respectively. The ENDF/B-VIII.0 evaluation is compared against data by Drake [28, 29] and Nellis [25]. Note that at 14.2 MeV incident neutron energy, we use corrected data from Drake available now in EXFOR. The double-differential cross section measured by both Drake and Nellis at select angles was integrated over all directions assuming isotropic emission (factor of  $4\pi$ ).

measured total gamma production spectrum, defined as

$$\frac{d\Sigma_{\gamma}(E_n; \varepsilon_{\gamma})}{d\varepsilon_{\gamma}} = \sum_c \langle \nu_{\gamma}^{(c)} \rangle (E_n) \sigma_c(E_n) \bar{\chi}_{\gamma}^{(c)}(E_n; \varepsilon_{\gamma}), \quad (4)$$

where  $c$  stands for all open channels that generate gamma-rays (*e.g.*, capture,  $(n, n')$ ,  $(n, 2n)$ , fission, *etc.*),  $\langle \nu_{\gamma}^{(c)} \rangle$  is the average multiplicity for channel  $c$ , and  $\bar{\chi}_{\gamma}^{(c)}(E_n; \varepsilon_{\gamma})$  is the average gamma-ray spectrum for channel  $c$ . While the experiments are performed at different angles, we have assumed isotropic emission of gamma-rays since not enough information is available to pin down an angular dependence for the channels involved. We will return to the problem of determining the average gamma multiplicity for fast neutrons in Sec. III A 2. The evalu-

ated differential cross section for the total gamma production is shown in Fig. 3 for 1 MeV and 14.2 MeV incident neutron energies, respectively. In both cases, the evaluation is in good agreement with the available experimental data [25, 28, 29]. It should be noted that Drake *et al.* incorrectly quoted the cross section for the energy bins above 4 MeV outgoing gamma-ray energy in Table II of Ref. [29]. This most likely was due to the increase in the energy bin size from 100 to 500 keV, resulting in a factor of 5 drop for the double differential cross section. Only recently EXFOR compilers contacted the author and corrected the corresponding EXFOR entries accordingly (including  $^{235,238}\text{U}$  and  $^{239}\text{Pu}$  among others). Note that the ENDF/B-VII.1 evaluated data (carried over from earlier versions of ENDF) follow the uncorrected data [29], and therefore drop by a factor 5 at 4 MeV, as illustrated by the dotted green histogram in the upper panel of Fig. 3.

## 2. Average PFG Multiplicity and the Multiplicity Probability Distribution

At thermal neutron incident energy, a number of experiments have been performed to measure the average PFG multiplicity. However, as it can be inferred from Fig. 4, a significant discrepancy exists between different measurements, even when corrections for the low-energy gamma threshold inherent to each experiment are applied (full symbols) based on the ENDF/B-VIII.0 PFGs. Even for the same energy threshold, there is a relatively large spread between measurements, as shown in Table I. In addition, as discussed in the previous section, even the same experimental group provided two data sets that are discrepant at low energies, with a big impact on the average PFG multiplicity. As the decision to use CGMF at low energies was based on the very good agreement with the 2013 PFGs by Oberstedt *et al.* [32], we have adopted 8.58 as the thermal average multiplicity. By applying the 100 keV correction cut, we obtain perfect agreement with the average multiplicity reported in Ref. [32]. As shown in Table I, for a 140 keV cut, the evaluated multiplicity remains larger than any of the other reported values, but it is in reasonable agreement to the DANCE measurement [36], and within Peelle's uncertainties. Note that all measurements have a very similar time-coincidence window, between 6 and 10 ns, so any dependence on this variable should be negligible.

At higher incident neutron energies, no direct measurements of the average PFG multiplicity are available for the  $^{235}\text{U}(n, f)$  reaction. So, in order to extract the average PFG multiplicity, we turn to data on the total cross section for gamma production, which is obtained by integrating over the outgoing gamma-ray energy in Eq. (4)

$$\Sigma_{\gamma} = \sum_c \langle \nu_{\gamma}^{(c)} \rangle \sigma_c, \quad (5)$$

where for simplicity the incident neutron energy  $E_n$  de-

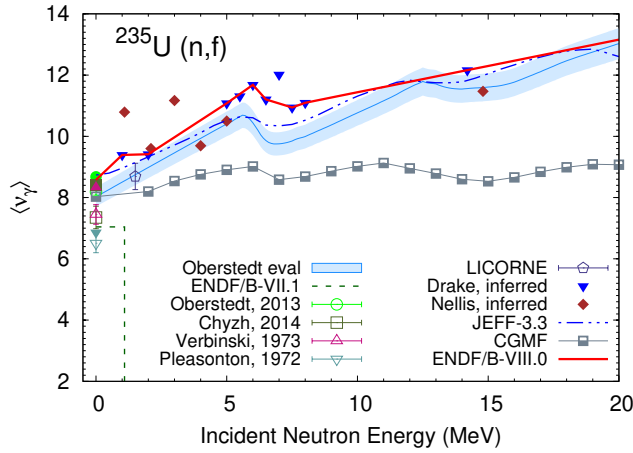


FIG. 4. (Color online) Average prompt fission gamma multiplicity as a function of incident neutron energy. With empty symbols we show the measured experimental data, while with full identical symbols we show the same data corrected according to the experimental range of outgoing gamma-ray energies, based on the ENDF/B-VIII.0 evaluation. The PFG multiplicity data was taken from Refs. [31, 32, 35, 36], while the inferred data was extracted from measurements of total gamma production cross section by Drake [28, 29] and Nellis [25]. The LICORNE datapoint at 1.5 MeV is taken from the analysis presented in Ref. [13]. The inferred multiplicity points were calculated according to Eq. (6) from the total gamma production cross section measured by Drake [28, 29], Nellis [25], and Gorbachev [43]. The shaded area shows the Oberstedt evaluation [13].

pendence explicitly shown for all quantities in Eq. (4) has been dropped, but should be understood. Only in the case of fission, we will suppress the channel name  $f$  for the average PFG multiplicity. Hence, assuming that the other channels are well modeled/evaluated, and especially when fission dominates the gamma production, we can extract the fission gamma multiplicity at different incident neutron energies by using existing Los Alamos measurements by Drake [28, 29] of the total gamma-ray production cross section

$$\langle \nu_\gamma \rangle = \frac{1}{\sigma_f} \left( \Sigma_\gamma - \sum_{c \neq f} \langle \nu_\gamma^{(c)} \rangle \sigma_c \right). \quad (6)$$

In order to match the existing data, we have taken into account the reported experimental energy range of the outgoing gamma-rays using extrapolations from the ENDF/B-VIII.0 PFGs, as shown in the lower panel of Fig. 5. The total gamma production cross section including gammas from 0 to 30 MeV is shown in the upper panel of the same figure. There we have also applied corrections based on ENDF/B-VIII.0 PFGs to the experimental data by Drake [28, 29] and Nellis [25]. In the lower panel, the data by Nellis is systematically lower than Drake, because the low-energy detection threshold is lower. Once the corrections using the ENDF/B-VIII.0

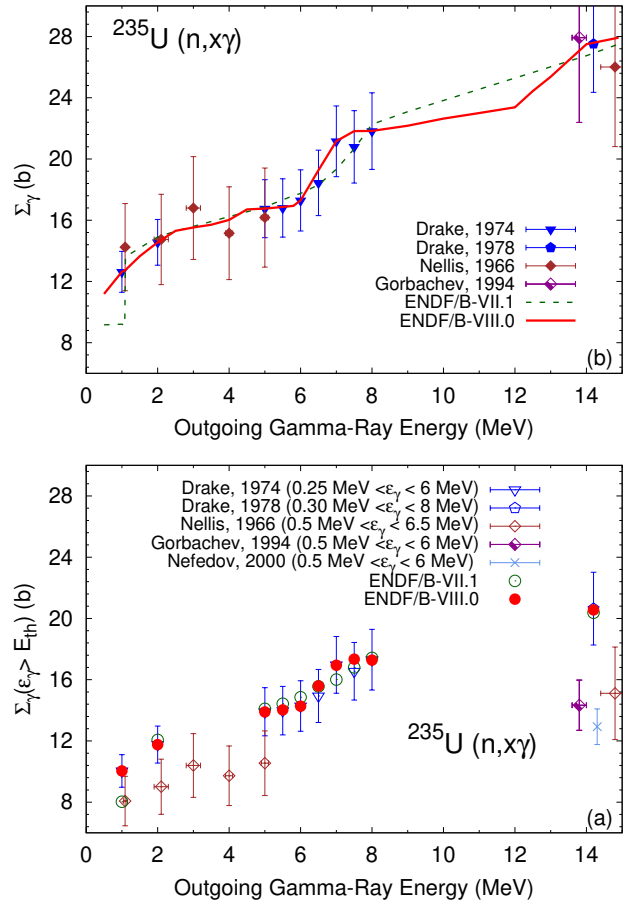


FIG. 5. (Color online) Total gamma production  $\Sigma_\gamma$  as a function of incident neutron energy. In the lower panel, the existing data are shown without any corrections, with the energy detection range shown in the legend for each experiment. The ENDF/B-VII.1 and ENDF/B-VIII.0 points are obtained using the energy ranges reported by Drake [28, 29], and do not take into account the Nellis [25] or Gorbachev [43] data in the evaluation. In the upper panel, we show the total gamma production cross section as a function of incident neutron energy, with all the gamma-rays included. The experimental data were corrected using ENDF/B-VIII.0.

evaluation are applied, both data sets become fairly consistent. Note that the data by Nellis [25] has not been used in the evaluation process.

The average PFG multiplicity as a function of incident neutron energy is shown in Fig. 4 and compared against available measured data and simulation results. Oberstedt *et al.* [13] predictions for the  $^{235}\text{U}(n,f)$  reaction show a lowering of the average PFG by about 3%, otherwise the same dependence of the incident neutron energy is observed [33]. As noted earlier, our evaluation uses the Drake data (except for the point at 7 MeV, which seems to be an outlier). CGMF simulations exhibit a much less pronounced increase of the average PFG multiplicity with respect to the incident neutron energy; the reasons for this difference are not yet understood. In these sim-

ulations, we have calculated the average multiplicity by imposing a cut of 100 keV, in order to remove the spurious gamma-rays from the calculation. However, such a cut produces only a small overall shift. As expected, small decreases in the average PFG multiplicity as a function of incident neutron energy are observed at different multi-chance fission thresholds.

In an effort to provide more detailed information useful in the simulation of certain integral experiments, a new format was introduced in the ENDF-6 manual to accommodate the storage of  $P(\nu_\gamma)$  and the multiplicity-dependent spectra for both prompt neutrons and gamma-rays. This new format was used in ENDF/B-VIII.0 to store only  $P(\nu_\gamma)$  for both neutrons and gamma-rays. We plan to store the multiplicity-dependent spectra in future updates of the evaluation.

The relation between the average PFGS and the multiplicity-dependent spectra for fixed incident neutron energy  $E_n$  is given by

$$\bar{\chi}(\varepsilon; E_n) = \frac{1}{\langle \nu \rangle(E_n)} \sum_{\nu > 0} \nu P(\nu; E_n) \bar{\chi}_\nu(\varepsilon; E_n), \quad (7)$$

where  $P(\nu, E_n)$  is the probability to emit  $\nu$  particles in a fission event and  $\bar{\chi}_\nu(\varepsilon; E_n)$  is the average spectrum for multiplicity  $\nu$ . While in principle measurements of the multiplicity-dependent spectra can be performed, few data currently exist. Indirect information about the multiplicity-dependent spectra based on a simplified model [38, 44] was extracted only for incident thermal neutrons. Hence, multiplicity-dependent spectra is available only from simulations at the moment. Equation (7) relates the average evaluated PFGS to the multiplicity-dependent spectra, which means that the simulated total PFGS has to agree to very high accuracy with the evaluated spectrum, in order to be able to use the theoretical results for the multiplicity-dependent spectra in evaluations. In addition, as discussed earlier, the average multiplicity obtained in simulations does not agree to high enough accuracy with the average multiplicity observed or extracted from the total gamma production data. Hence, the evaluation of the multiplicity-dependent PFGS was not included in the ENDF/B-VIII.0 evaluation. In the future, we plan to enforce Eq. (7) either by performing adjustments to the multiplicity-dependent spectra, or by tuning the simulations to better reproduce the evaluated average PFGS.

The PFG multiplicity probability distribution was evaluated using both experimental input and simulations. We have noted in our previous publications [10, 45] that the CGMF calculations can be fitted with very high accuracy by the negative-binomial model introduced by Valentine [39, 40]

$$P(\nu_\gamma) = \binom{\beta + \nu_\gamma - 1}{\nu_\gamma} p^\beta (1-p)^{\nu_\gamma}, \quad (8)$$

where  $\beta$  is a parameter related to the width of the distribution, and  $p$  is a parameter related to both the mean

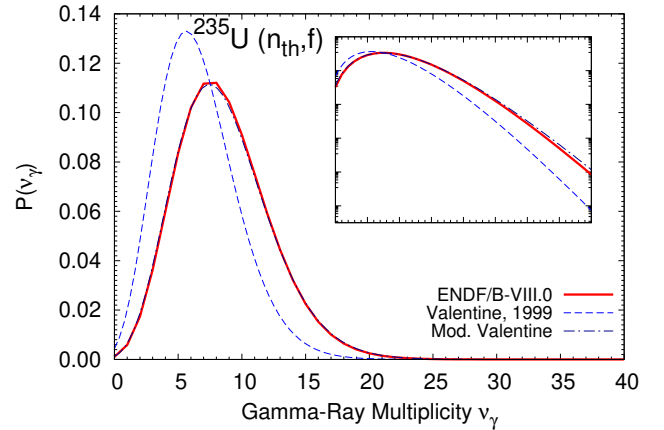


FIG. 6. (Color online) The gamma-ray multiplicity probability distribution for the induced fission of  $^{235}\text{U}$  with thermal neutrons. We also present the double poisson distribution of Valentine [39, 40] (dashed line) and a modified version of the Valentine parameterization, where the average multiplicity was set to the current ENDF/B-VIII.0 value of 8.58 (dash-dotted line). The modified parameters for the negative binomial are  $\beta = 14.29$  and  $p = 0.63$ . In the insert, the same distributions are plotted on logarithmic scale.

and the width of the distribution  $\langle \nu_\gamma \rangle$ ,

$$p = \frac{\beta}{\beta + \langle \nu_\gamma \rangle}. \quad (9)$$

We have fitted the parameters  $\beta$  and  $p$  to the CGMF simulations as a function of incident neutron energy. However, because the average PFG multiplicity calculated with CGMF as a function of incident energy does not reproduce the evaluated average multiplicity (see Fig. 4), we have replaced the CGMF value of the average multiplicity in Eq. (9) by the evaluated values discussed above. Because at the moment the ENDF-6 manual only allows a tabulated format for  $P(\nu_\gamma)$ , we have generated numerical values for the multiplicity probability using the negative binomial functional form in Eq. (8). In Fig. 6, we show the multiplicity probability estimated by Valentine [39] (dashed line) based on experiments that have 100 keV threshold for gamma-ray detection, and the ENDF/B-VIII.0 evaluation. If the negative binomial parameters of Valentine are modified so that the average PFG multiplicity matches the ENDF/B-VIII.0 value, we obtain excellent agreement with the current evaluation, where the width is extracted from the CGMF calculations ( $\beta = 14.29$ ,  $p = 0.63$ ).

For a normalized probability distribution  $P(\nu_\gamma)$ , the second and third factorial moments are defined as

$$\langle \nu_\gamma(\nu_\gamma - 1) \rangle = \sum_{\nu_\gamma} \nu_\gamma(\nu_\gamma - 1) P(\nu_\gamma), \quad (10)$$

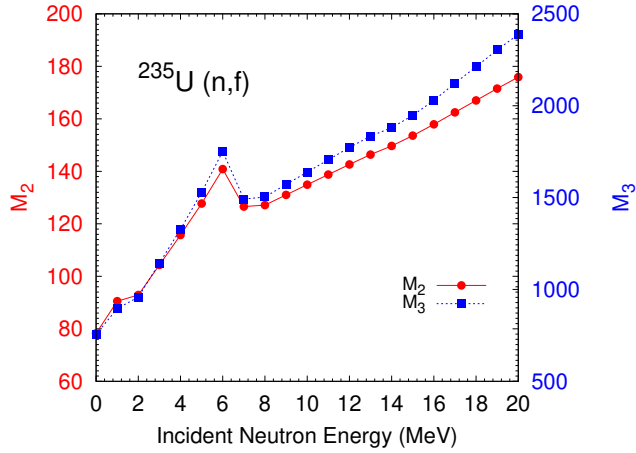


FIG. 7. (Color online) Second (filled circles) and third (filled squares) factorial moments using the ENDF/B-VIII.0 gamma-ray multiplicity probability as a function of energy. The left axis corresponds to the second moment, while the right axis to the third moment. See text for definition of the factorial moments.

and

$$\langle \nu_\gamma(\nu_\gamma - 1)(\nu_\gamma - 2) \rangle = \sum_{\nu_\gamma} \nu_\gamma(\nu_\gamma - 1)(\nu_\gamma - 2)P(\nu_\gamma), \quad (11)$$

respectively. Both moments are plotted in Fig. 7, but unfortunately no data are available for comparison.

### 3. Average Total PFG Energy

In ENDF/B-VIII.0, the format was changed in file 1 to allow for tabulated values of the average PFG energy released as a function of incident neutron energy. This quantity is defined in the evaluation as the product of the average photon energy and the average multiplicity. In Table I, we compare available data with the evaluation, for thermal neutrons. In Fig. 8, we compare the evaluated total PFG energy released as a function of incident neutron energy with other evaluations (including ENDF/B-VII.1) and other experimental data. Most of the available experimental data are for thermal neutron-induced fission, and only the data by Fréhaut are available for an incident energy range from about 1 to 15 MeV [46]. The documentation for this data set is rather poor, but it was employed by Madland to perform a linear fit [47], which was used in ENDF/B-VII as an evaluation of the total gamma energy released. The CGMF results are relatively close to the Fréhaut data up to about 11 MeV, but show a more pronounced dip at the threshold for second-chance fission. The Fréhaut CEA data does not seem to show any significant feature at the threshold for third-chance fission, while CGMF displays a decrease with incident energy between 11 and 15 MeV. Both

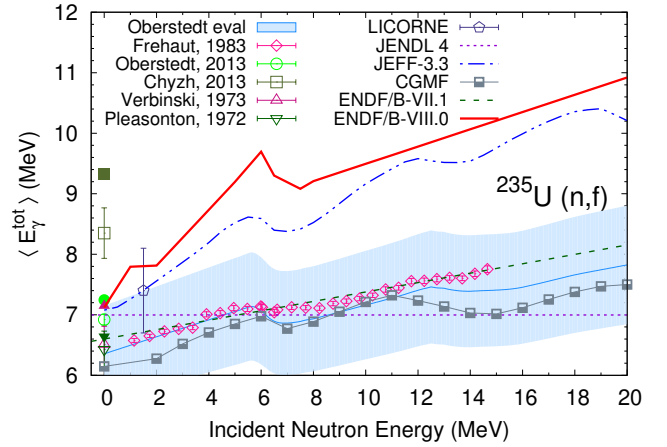


FIG. 8. (Color online) The average total PFG energy per fission event as a function of the incident neutron energy for the  $^{235}\text{U}(n,f)$  reaction. As in Fig. 4, with empty symbols we show the measured experimental data, while with full identical symbols we show the same data corrected according to the experimental range, based on the ENDF/B-VIII.0 evaluation. Because the threshold for the Fréhaut measurement [46] is not available, no threshold correction has been applied for this dataset. The thermal data were taken from Refs. [31, 32, 35, 36], while the LICORNE result was reported in Ref. [13]. The shaded area shows the ENDF/B-VIII.0 evaluation [13]. In the 1 – 20 MeV range, ENDF/B-VIII.0 lies above the other evaluations because it is based on Drake’s data, see Figs. 3 and 4.

CGMF and the Fréhaut data are significantly below the ENDF/B-VIII.0 evaluation, based on the average multiplicity extracted from the Drake total production data and the average photon energy at thermal incident energy. JEFF-3.3 is closer to ENDF/B-VIII.0, and is based on the model published in Ref. [14], in which the average multiplicity is linearly connected with the average number of neutrons emitted from fission fragments. The discrepancy between Fréhaut and the ENDF/B-VIII.0 evaluation, which is based on the Drake data, is not yet understood.

## B. The $^{238}\text{U}(n,f)$ Reaction

Even fewer data are available for the  $^{238}\text{U}(n,f)$  reaction than for the  $^{235}\text{U}(n,f)$  reaction discussed in the previous section. Hence, in the evaluation of the  $^{238}\text{U}(n,f)$  PFG properties, some missing information has been replaced with data from the  $^{235}\text{U}(n,f)$  reaction, assuming that the two reactions are similar, as suggested by Ref. [48].

Given the scarcity of data, including data on total gamma production, we have assumed that the average PFG multiplicity for the  $^{238}\text{U}(n,f)$  reaction has the same incident neutron energy dependence as for  $^{235}\text{U}(n,f)$ . An overall multiplicative factor with respect to the  $^{235}\text{U}(n,f)$  was fixed so that the Drake total gamma production at

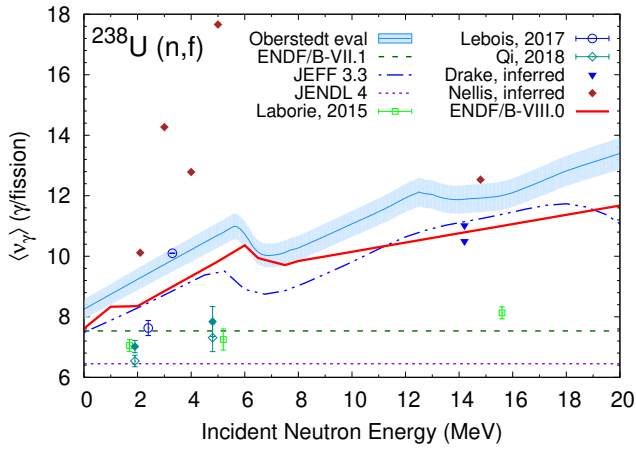


FIG. 9. (Color online) Same as in Fig. 4, but for the  $^{238}\text{U}(n,f)$  reaction. The Lebois, 2017 datapoints and the 15.6 MeV Laborie, 2015 result have been digitized from Ref. [14], while the measurements at 1.7 and 5.2 MeV were taken from Table III in Ref. [49], which also reported the data at 1.9 and 4.8 MeV. The inferred multiplicity points were calculated according to Eq. (6) from the total gamma production cross section measured by Nellis [25] and Drake [29]. The shaded area shows the Oberstedt evaluation [13, 14].

14.2 MeV incident neutron energy [29] is well reproduced. The average PFG multiplicity as a function of energy for  $^{238}\text{U}(n,f)$  is shown in Fig. 9. In this case, the ENDF/B-VIII.0 evaluation is closer to the latest JEFF-3.3 evaluation [50], while still slightly below the Oberstedt evaluation [14]. All available experimental data [24, 49] suggest a weak increase of the multiplicity with the incident neutron energy. However, this behavior is hard to reconcile with the  $^{235}\text{U}(n,f)$  data by Fréhaut, which was interpreted as an increase in the fission fragment spin with increasing incident neutron energy. The same more pronounced increase with the incident neutron energy as in Fréhaut data was observed in CGMF simulations [11]. This increase in the average spin translates naturally into an increase in the average PFG multiplicity, as more electromagnetic transitions are required in order to match the lower spins of the low-lying states.

Below 1 MeV outgoing gamma-ray energy, the PFGS was evaluated using the JEFF-3.3 spectrum, which was based on a recent experiment by Lebois *et al.* [48]. Above 1 MeV gamma-ray energy, the  $^{235}\text{U}(n,f)$  PFGS was adopted. The same assumption of no incident neutron energy dependence was made, so that the average total gamma-ray energy is proportional with the multiplicity. In Fig. 10 the evaluated PFGS is compared with the data by Lebois *et al.* [48], and our CGMF simulations. By comparison with the data, the agreement is good up to about 3.5 MeV, and at higher energies the evaluation becomes softer. However, it is possible that the errors are underestimated, given that only the ratio  $^{235}\text{U}/^{238}\text{U}$  could be precisely measured [48]. The CGMF results are close to the evaluation, but fewer gamma-rays are pro-

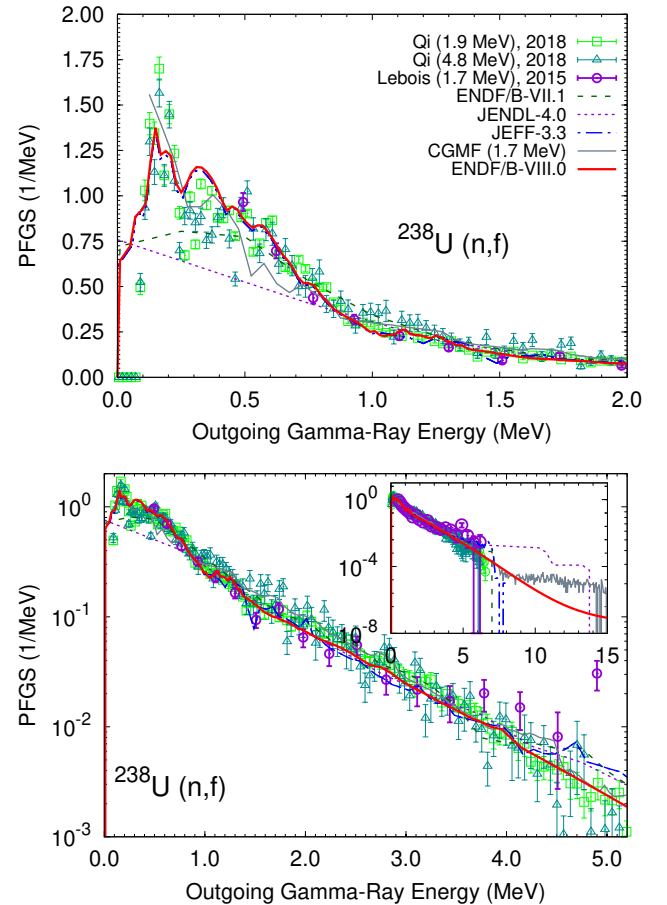


FIG. 10. (Color online) Same as in Fig. 2, but for the  $^{238}\text{U}(n,f)$  reaction. The experimental PFGS has been measured at different incident neutron energies (1.7 [48], 1.9, and 4.8 MeV [49]). The CGMF calculation has been performed at 1.7 MeV incident neutron energy, while the evaluated spectra are incident neutron energy independent.

duced in the 250 to 750 keV interval. Hence, after the normalization to 1, the CGMF spectrum lies slightly above the evaluation at outgoing gamma-ray energies higher than 1 MeV. Note that because of a relatively high detection threshold (about 400 keV) of the  $\text{BaF}_2$  detectors, no reliable multiplicities could be extracted in this experiment [48]. More recent data by Qi *et al.* [49] at 1.9 and 4.8 MeV incident neutron energies show a larger spread at low outgoing gamma-ray energies, but a relatively good agreement with CGMF, especially above 2 MeV.

In Fig. 11, we plot the evaluated average total PFG energy as a function of incident energy, and compare it against older evaluations, and simulations by Tudora *et al.* [20] in the point-by-point model [51, 52], and the latest Oberstedt evaluation [14]. Unlike for the  $^{235}\text{U}(n,f)$  reaction, the ENDF/B-VIII.0 evaluation is within the (large) uncertainties of the Oberstedt evaluation, even though the shape is different from the central values obtained by the authors. Furthermore, above the threshold for second-chance fission, the evaluation is fairly close to the

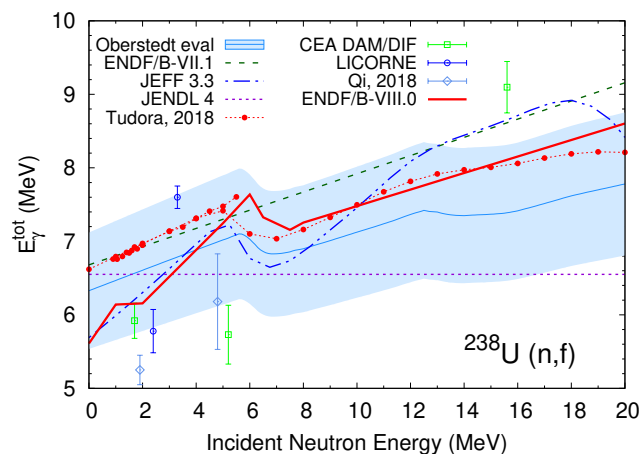


FIG. 11. (Color online) Same as in Fig. 8, but for the  $^{238}\text{U}(n,f)$  reaction. As in Fig. 9, the Lebois, 2017 datapoints and the 15.6 MeV Laborie, 2015 result have been digitized from Ref. [14], while the measurements at 1.7 and 5.2 MeV were taken from Table III in Ref. [49], which also reported the data at 1.9 and 4.8 MeV. The shaded area shows the Oberstedt evaluation [13, 14]. The model calculations by Tudora, made available to us in 2018, have not been published by the author, but included in Ref. [14].

values predicted by Tudora *et al.* [51].

The total gamma production as a function of the incident neutron energy is shown in Fig. 12, calculated within the range of outgoing gamma-ray energies measured in each available experiment (lower panel) and from zero to 30 MeV outgoing gamma-ray energy, with the experimental data corrected for the missing contributions (upper panel). Thus, while the agreement between the total gamma production measured by Nellis is not great below 6 MeV, the evaluation for most incident neutron energies falls within the quoted uncertainties. The data by Filatenkov [53] at 3 MeV incident neutron energy, measured between 0.25 and 3.55 MeV outgoing gamma-ray energies, are, to some extent, consistent with the Nellis data, while the data by Nefedov [54] seems to overestimate the total gamma production by comparison to Drake and Nellis at neighboring incident neutron energies.

In Fig. 12, the evaluated total gamma production is within or just outside the uncertainties of the experimental data, which would imply that the multiplicity extracted from the Nellis data using Eq. (6) would be in reasonable agreement with the evaluated ENDF/B-VIII.0 multiplicity. Below 6 MeV neutron incident energy, a serious discrepancy between Nellis and the evaluation can be observed in Fig. 9. In particular, the total production data at 2 MeV is in excellent agreement with the measured data, but the multiplicity is more than 20% higher than the evaluation, and for higher incident neutron energies the situation is worse still. In order to understand the discrepancy, we plot in Fig. 13 the contribution from different open reaction channels, including fission, at 1.09,

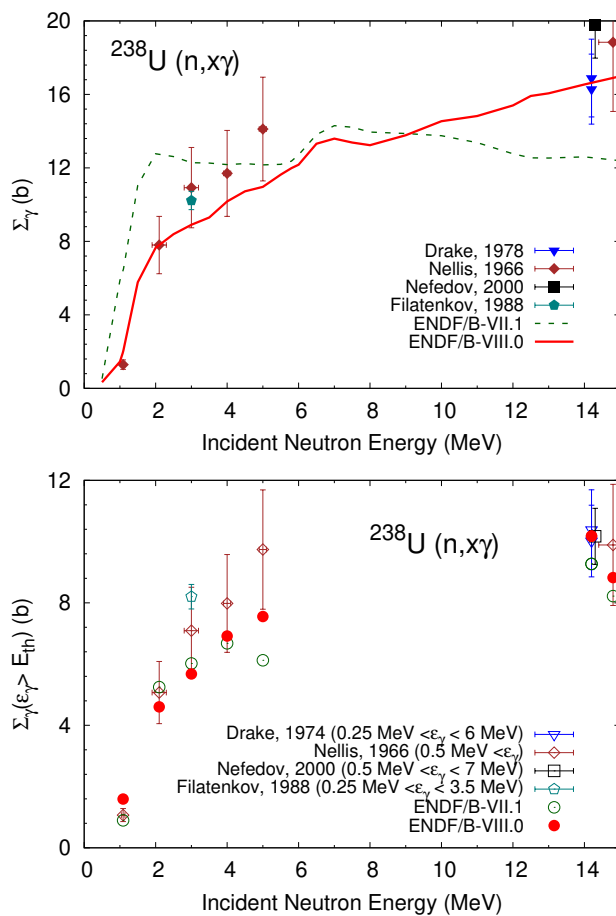


FIG. 12. (Color online) Same as in Fig. 5, but for the  $^{238}\text{U}(n,f)$  reaction. The data were taken from Refs. [25, 29, 53, 54].

3.0, 5.0, and 14.2 MeV incident neutron energies and compare against available data. At most energies, the total production spectrum data agree reasonably well with the evaluation. However, in contrast with the  $^{235}\text{U}(n,f)$  reaction, where fission dominates the gamma production at all incident neutron energies (see Fig. 3), different channels contribute significantly to the total cross sections, even at high incident neutron energies [55]. Thus, at 1.09 MeV the capture channel dominates at outgoing gamma-ray energies above 1 MeV, while below 1 MeV the  $(n,n')$  channel gives most of the contribution. At 3 and 5 MeV, the fission competes with  $(n,n')$ , while at 14.2 MeV, a significant contribution comes from the  $(n,2n)$  channel. Hence, the multiplicity extraction from the total production data is subject to uncertainties in the evaluation of other channels. The errors can be minimized only when fission dominates. Finally, the 1.09 MeV data presented in Fig. 13 (upper left panel) strongly suggest that the evaluation of the capture channel [55] should be revisited for the next release of the library, considering the fact that  $^{238}\text{U}$  capture is evaluated with Neutron Data Standards up to 2 MeV [56].

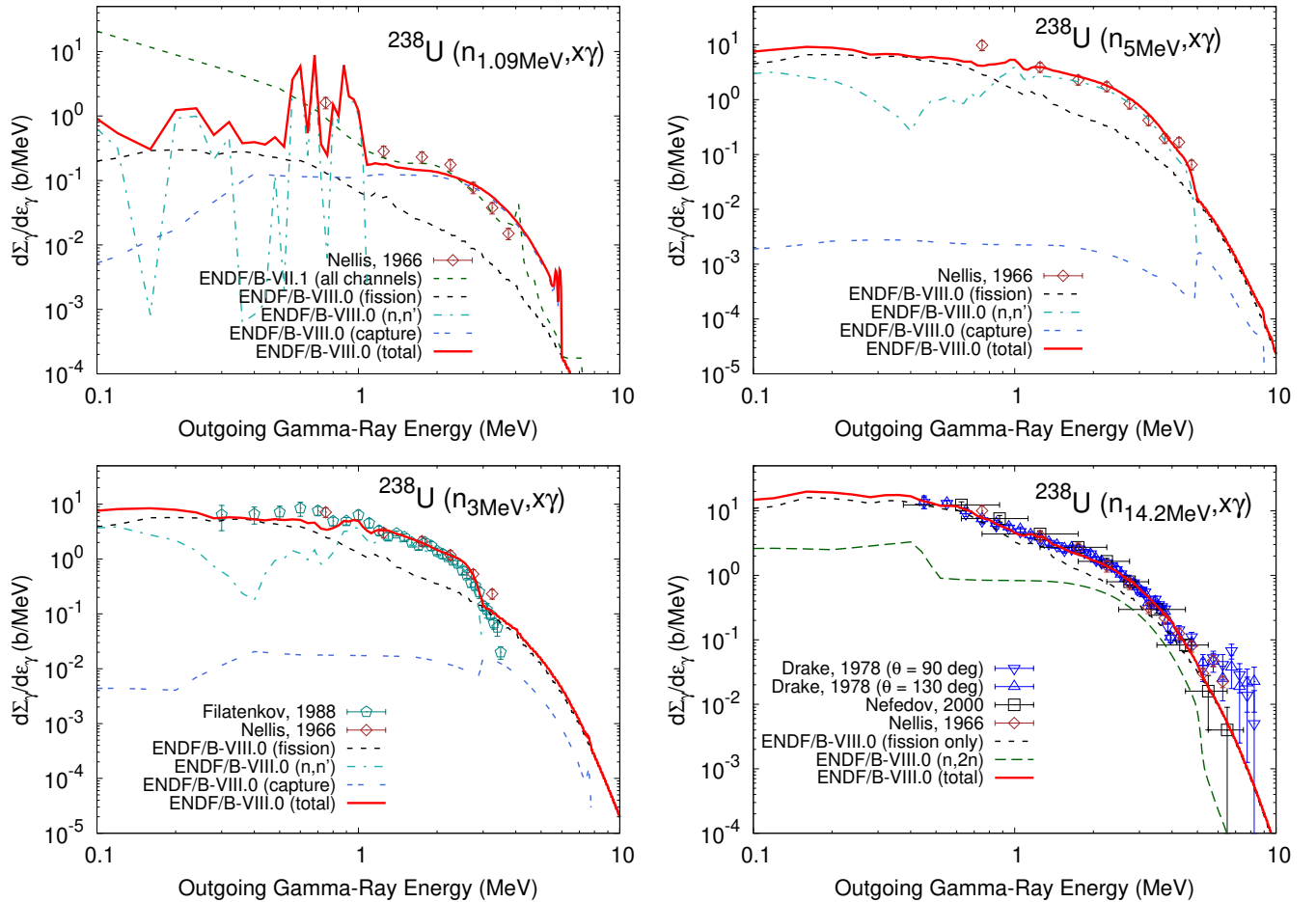


FIG. 13. (Color online) Total gamma production spectrum as a function of the outgoing gamma-ray energy, for 1.09, 3, 5 and 14.2 MeV neutron incident energies. As in Fig. 3, the corrected 14.2 MeV incident neutron energy data available in EXFOR was used instead of the original data from Ref. [29]. The Nellis data at all incident energies shown were taken from Ref. [25], and Filatenkov data at 3 MeV from Ref. [53]. As in Fig. 3, the corrected 14.2 MeV incident neutron energy data available in EXFOR was used. For all the experiments where the double-differential cross section was measured at select angles, we integrated over all directions assuming isotropic emission (factor of  $4\pi$ ). Note that small differences appear for the measurements by Drake at two different angles, but they are consistent within quoted uncertainties. Thus, while we do not discount the possibility of an anisotropy, the data are also consistent with isotropic emission.

The PFG multiplicity distribution probability has been constructed using the same procedure as for the  $^{235}\text{U}(n,f)$  reaction, using the evaluated  $^{238}\text{U}(n,f)$  prompt gamma-ray multiplicity. For the width, given the absence of the experimental data and problems with the implementation of the incident neutron energy dependence for  $^{238}\text{U}$  in CGMF at the time of the evaluation, we have used the same width as for the  $^{235}\text{U}(n,f)$  reaction. The results for the factorial moments are presented in Fig. 14.

A summary of the PFG properties for the  $^{238}\text{U}(n,f)$  reaction compared against available experimental data and simulations is presented in Table II, where we have also included the recently published data from the CEA by Qi *et al.* [49]. The last reference also contains values for average PFG multiplicities, average photon energies, and total gamma-ray energy released discussed, but not explicitly given in Ref. [24]. It can be observed

that all measurements are in reasonable agreement regarding the average photon energy, and consistent within the uncertainties with the ENDF/B-VIII.0 evaluation of  $\langle\varepsilon_\gamma\rangle = 0.79$  MeV for a 100 keV energy measurement threshold. Note that the authors in Ref. [48] say that, while the detectors have a rather high detection threshold for gamma-rays (about 400 keV), they apply a correction that should push the detection threshold down closer to 100 keV. The measured average PFG multiplicity and the average total gamma-ray energy released are consistently lower than the evaluation, but different experiments are also somewhat inconsistent with each other. A possible explanation would be that the Drake data used in the evaluation is inconsistent with the more recent measurements.

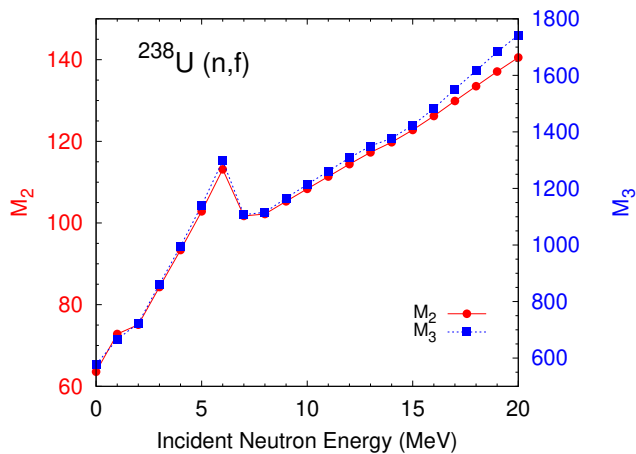


FIG. 14. (Color online) The same as in Fig. 7, but for the  $^{238}\text{U}(n,f)$  reaction.

TABLE II. Evaluation of prompt fission gamma-ray properties: comparison between the current evaluation, experimental data and CGMF for  $^{238}\text{U}(n,f)$ . For comparison with available measured data, we also show the CGMF calculation at 1.7 incident neutron energy, with the corresponding emission threshold energy  $E_{\text{thresh}} = 100$  keV. Higher incident energies recently reported have also been included. The low-energy emission threshold  $E_{\text{thresh}}$  is given in keV, the while all the other energies are in MeV. The data by Lebois *et al.* [48] was obtained with 400 keV threshold detectors, but further corrections during the analysis suggest a measurement equivalent to 100 keV threshold.

	$E_{\text{thresh}}$	$\langle\nu_{\gamma}\rangle$	$\langle\varepsilon_{\gamma}\rangle$	$\langle E_{\gamma}^{\text{tot}}\rangle$
ENDF/B-VIII.0	0	7.61	0.74	5.61
ENDF/B-VII.1		7.53	0.89	6.68
JEFF-3.3		7.49	0.76	5.68
JENDL 4		6.45	0.97	6.22
ENDF/B-VIII.0 (1.7 MeV)	0.1	7.78	0.79	6.12
ENDF/B-VII.1 (1.7 MeV)	0.1	7.04	0.94	6.65
CGMF (1.7 MeV)	0.1	8.50	0.76	6.46
Laborie (1.7 MeV) [24]	0.1	7.05(20)	0.84(3)	5.92(24)
Lebois (1.7 MeV) [48]	0.1	7.59	0.77(6)	
ENDF/B-VIII.0 (1.9 MeV)	0.1	7.78	0.79	6.12
Qi (1.9 MeV) [49]	0.1	6.54(19)	0.80(4)	5.25(20)
ENDF/B-VIII.0 (4.8 MeV)	0.1	9.07	0.79	7.13
Qi (4.8 MeV) [49]	0.1	7.31(46)	0.84(11)	6.18(65)
ENDF/B-VIII.0 (5.2 MeV)	0.1	9.26	0.79	7.29
Laborie (5.2 MeV) [24]	0.1	7.25(35)	0.79(4)	5.73(40)

### C. The $^{239}\text{Pu}(n,f)$ Reaction

The evaluation of the prompt fission gamma produced in the neutron-induced fission of  $^{239}\text{Pu}$  follows a similar procedure to the one used for  $^{235}\text{U}(n,f)$ . The available available experimental information on the PFGS and PFG multiplicity was used at thermal, while CGMF simulations, and data on total gamma production for fission induced by fast neutrons.

The new evaluation of the PFGS is based on the most

recent measurement by the Geel group at the Budapest Neutron Centre [57] below 2 MeV outgoing gamma-ray energy. Above 2 MeV, we have used CGMF calculations (Monte-Carlo and deterministic modes), which allowed us to extend the evaluation up to 20 MeV outgoing gamma-ray energies. As for the other two reactions, the evaluated PFGS is taken to be independent of the incident neutron energy. The multiplicity data of Ref. [57] lies between the recent data measured at Los Alamos by Chyzh *et al.* [36, 41] and Ullman *et al.* [44].

In Fig. 15 we compare the ENDF/B-VIII.0 evaluation with existing experimental data as well as with the CGMF simulation results. In the evaluation we have used a coarser grid than in the experimental data of Gatera [57], which explains some of the small discrepancies between the evaluation and this experimental set. The locations of the peaks produced by the discrete transitions in fission fragments are well reproduced in CGMF calculations below 1 MeV. On the other hand, some strength is missing and some is redistributed below 1 MeV from the CGMF calculations as compared with experiment and the evaluation. As data on discrete transitions can be incomplete, it is conceivable that better agreement can be found in the future using libraries that include improved experimental data and levels and discrete transitions. Above 1 MeV, the evaluation is in reasonable agreement with Gatera *et al.* and the Bayesian unfolded data by Chyzh *et al.* [41]. Up to about 4 MeV, it also reproduces relatively well the Verbinski data [35], but above 4 MeV the evaluation becomes softer. The Verbinski data set is also harder than the latest Budapest experiment [57].

The evaluated average PFG multiplicity is shown in Fig. 16, and compared against the available experimental data and CGMF simulations. Most of the experimental results are at thermal neutron incident energy, for different detector thresholds for gamma detection. For a meaningful comparison, we have corrected for detector threshold in Fig. 16 (full symbols), but also plotted the reported experimental results (empty symbols). At thermal incident energy, the average PFG multiplicity has been adjusted to reproduce the latest result by Gatera [57], when the 100 keV detector threshold is taken into account in the PFGS. The discrepancy between the measured PFG multiplicities reported by different groups at thermal incident energy is much smaller than for the  $^{235}\text{U}(n,f)$  reaction, so they are all in reasonable agreement with the evaluated data, as well as with the CGMF simulations.

As for the fission reactions on uranium isotopes included in this paper, there is a lack of data for fast neutrons and, hence, a similar procedure of using the total gamma production data was adopted. The experimental total gamma production cross section is shown in Fig. 17, and the PFG multiplicity was evaluated using Eq. (6) so that the measurement of Drake is reproduced. From 7 to 20 MeV incident neutron energy, we assumed a linear dependence of the average multiplicity, see Fig. 16, even though the CGMF simulations display a different trend. As in the case of  $^{238}\text{U}(n,f)$  reaction, the average PFG mul-

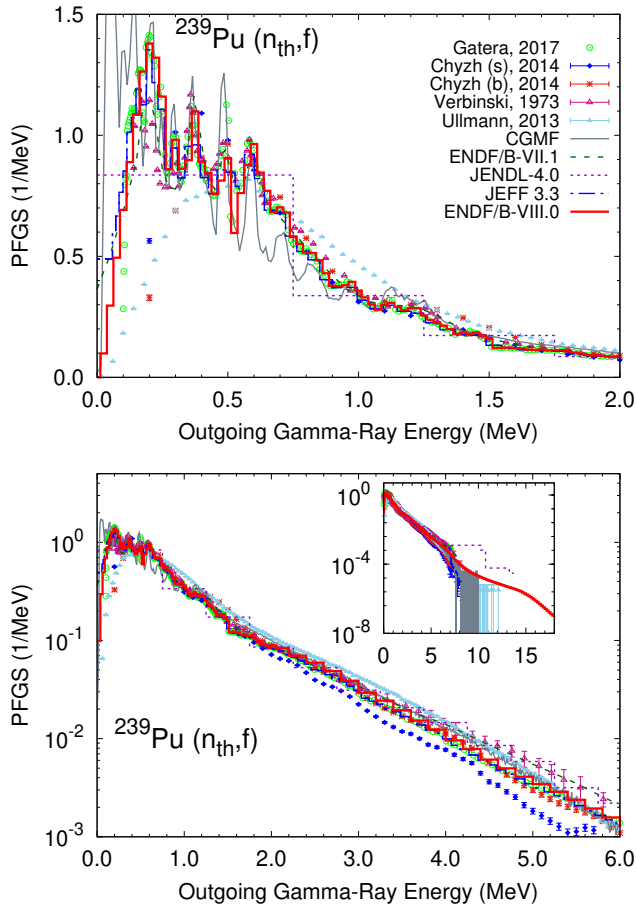


FIG. 15. (Color online) Same as in Fig. 2, but for the  $^{239}\text{Pu}(n_{\text{th}},f)$  reaction. We show the latest data by Gatera *et al.* [57], and older data by Verbinski [35], Chyzh *et al.* [36] (s/b stands for SVD/Bayesian method for unfolding the detector response), and Ullman *et al.* [44].

tiplicity extracted from the Nellis data is somewhat inconsistent with the evaluation. However, we note that total gamma production uncertainties are significant (about 20%), and that within the uncertainties the evaluation, the Drake data and the Nellis data are consistent, with the exception of the point at 3 MeV, where the evaluation is just outside the Nellis uncertainties (see the upper panel of Fig. 17).

Overall, a reasonable agreement between the evaluated gamma production spectra and experiment is shown in Fig. 18, due not only to the fact that Drake's total production data has been used in the evaluation procedure, but also because fission dominates the gamma production. Still, it is noteworthy that the *shape* of the ENDF/B-VIII.0 spectra in Fig. 18 agrees with the Drake and Nellis shapes, since the shape of the ENDF/B-VIII.0 PFGs was not adjusted to these experimental sets. As for the  $^{235}\text{U}(n,f)$  reaction, the excellent reproduction of the measured total gamma production spectrum at different energies (see Fig. 18 upper and lower panel) suggests a

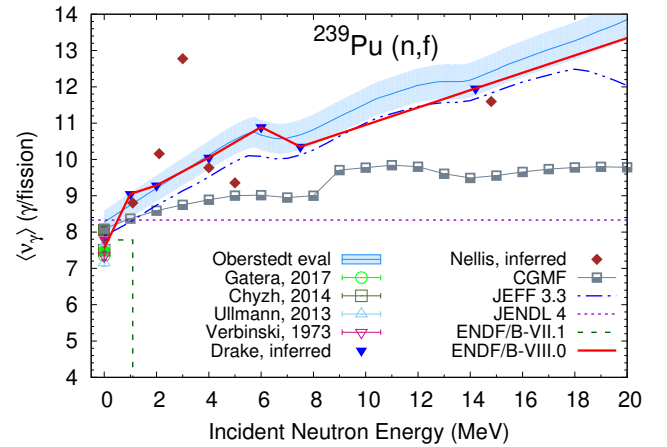


FIG. 16. (Color online) Same as in Fig. 4, but for the  $^{239}\text{Pu}(n,f)$  reaction. We compare against direct measurements by Verbinski [35], Ullmann [44], Chyzh [36] and Gatera [57] at thermal incident energy. The inferred multiplicity points were calculated according to Eq. (6) from the total gamma production cross section measured by Nellis [25] and Drake [27–29]. The shaded area shows the Oberstedt evaluation [58].

weak dependence for the average PFGs on the incident neutron energy.

The average total gamma-ray energy has been calculated as a product between the average PFG multiplicity, which depends on the incident neutron energy, and the average photon energy, assumed independent of the incident neutron energy. The comparison between the current evaluation and available experimental data is shown in Fig. 19, where we also plot an available evaluation by Fort [59]. The discrepancy between Fort and ENDF/B-VIII.0 evaluations is not understood at the moment. The non-smooth incident neutron energy dependence at 1 MeV is due to the fact that some of the current applications require a good reproduction of the total gamma production at this energy, compounded to the fact that no other measurements are available at or around this incident energy. The evaluation introduced by Oberstedt *et al.* [14, 58] produces values that are much lower than the current evaluation, even though a much better agreement can be observed for the average PFG multiplicity in Fig. 16.

Exactly the same method presented in Sec. III A 2 for the  $^{235}\text{U}(n,f)$  reaction has been used to evaluate  $P(\nu_\gamma)$ . Thus, the evaluated average PFG multiplicity was used in Eqs. (8), (9) to perform a fit of the parameter  $\beta$  to the widths of the distribution extracted from CGMF calculations for the  $^{239}\text{Pu}(n,f)$  reaction. Then the evaluated PFG multiplicity probability was generated using Eq. (8) as a function of incident energy. The second and third factorial moments of the distribution are shown in Fig. 20.

A summary of the PFG properties for the induced fission of  $^{239}\text{Pu}$  with thermal neutrons is presented in Table III. The agreement with experimental data is mixed.

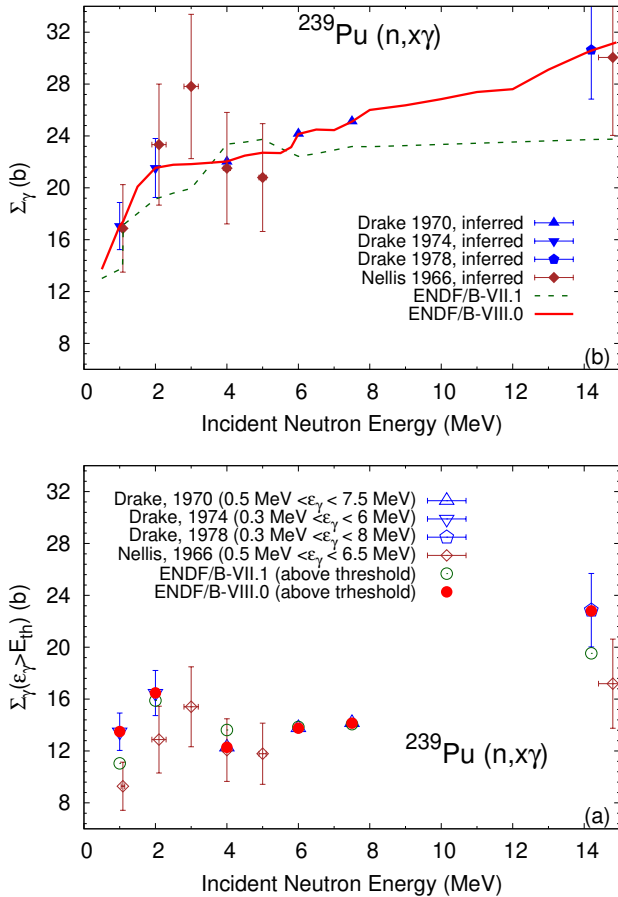


FIG. 17. (Color online) Same as in Fig. 5, but for the  $^{239}\text{Pu}(n,f)$  reaction. For comparison, we show the total gamma production cross section measured by Nellis [25] and Drake [27–29].

Thus, since the PFG multiplicity and spectrum evaluations are based on the Gatera *et al.* measurement [57], it is not surprising that the evaluation agrees well in terms of average PFG energy released. However, while the Verbinski [35] PFG multiplicity agrees with the evaluation within the measurement’s uncertainties, the PFGs in ENDF/B-VIII.0 is softer than the experiment, and hence the average PFG energy is about 0.5 MeV below Verbinski’s quoted value, and similarly for Ullmann *et al.* [44]. In the case of the Pleasonton data [60], the evaluations are just outside the quoted uncertainties for both PFG multiplicity and total PFG energy release, while the measured PFGs is significantly harder. Finally, the data by Chyzh *et al.* [36] overestimates the evaluations by 10 to 12%. CGMF reproduces the evaluation of the average PFG multiplicity within 3% and the evaluation of the total PFG energy released within 7%.

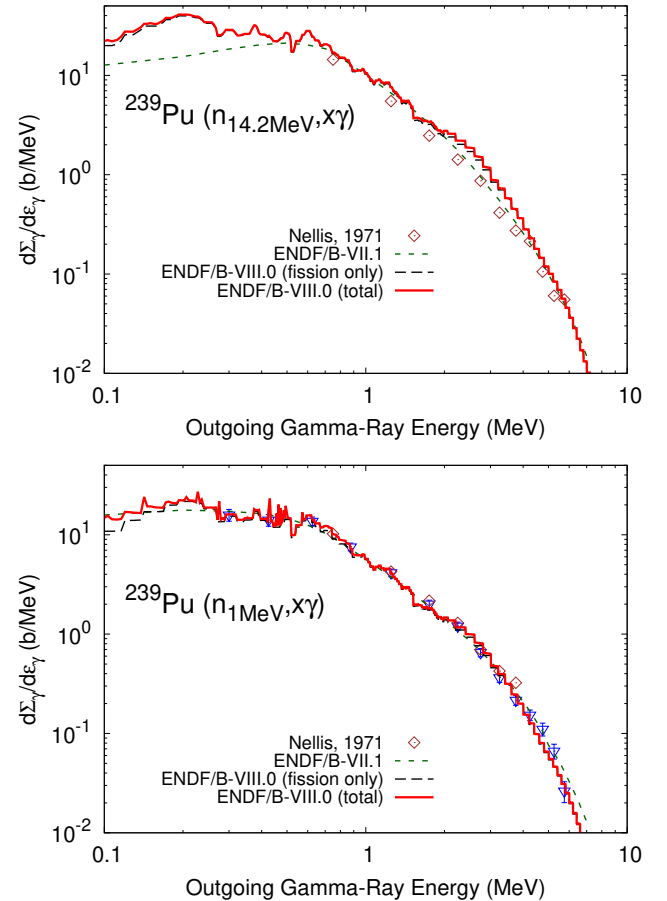


FIG. 18. (Color online) Total gamma production energy spectrum as a function of the outgoing gamma-ray energy, at 1 and 14.2 MeV neutron incident energies. For comparison, we show the total gamma production cross section spectrum measured by Nellis [25] at 1 and 14.8 MeV, respectively, and Drake [28] at 14.2 MeV. As in Fig. 3, the corrected 14.2 MeV incident neutron energy data available in EXFOR was used. For the experiments where the double-differential cross section was measured at select angles, we integrated over all directions assuming isotropic emission (factor of  $4\pi$ ).

#### IV. CONCLUSIONS AND OUTLOOK

We have presented details of the ENDF/B-VIII.0 evaluation of the prompt fission gamma produced in the neutron induced fission of  $^{235,238}\text{U}$  and  $^{239}\text{Pu}$ , for incident neutron energies from thermal to 20 ( $^{239}\text{Pu}$ ) or 30 MeV ( $^{235,238}\text{U}$ ). The main improvement in the current version of the library is the breakdown of the total gamma production into contributions from all channels that produce gamma-rays, including fission, with modifications informed by recent experiments. Thus, it is straightforward to replace in simulations the evaluation with fission event generators like CGMF or FREYA [4], which are already distributed with MCNP 6.2 [5].

The evaluation is based on input from available experimental data and model simulations using the CGMF code.

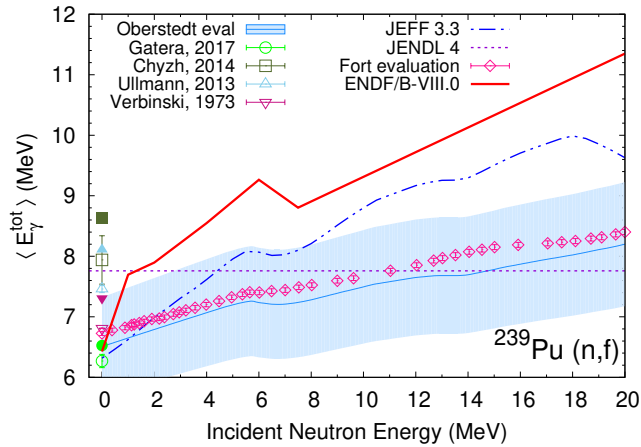


FIG. 19. (Color online) Same as in Fig. 8, but for the  $^{239}\text{Pu}(n,f)$  reaction. We show the latest data by Gatera *et al.* [57], and previously measured data by Verbinski *et al.* [35], Chyzh *et al.* [36], and Ullman *et al.* [44]. The shaded area shows the Oberstedt evaluation [58]. In the 1 – 20 MeV range, ENDF/B-VIII.0 lies above the other evaluations because it is based on Drake’s data, see Figs. 16 and 18 .

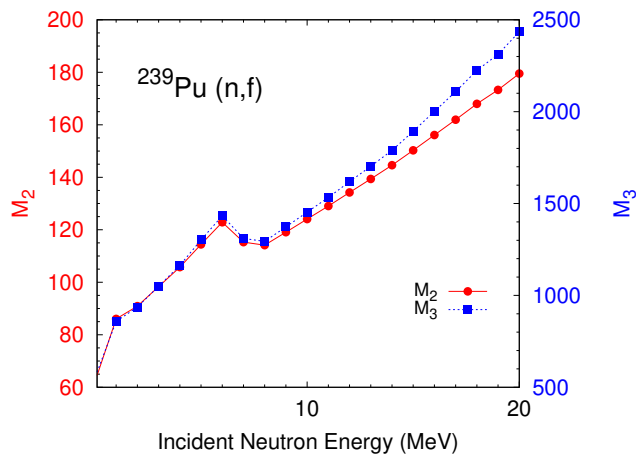


FIG. 20. (Color online) The same as in Fig. 7, but for the  $^{239}\text{Pu}(n,f)$  reaction.

A host of experimental PFG data are available mostly for thermal neutrons, while for fast neutrons, only limited experimental results are available, and mostly on total gamma production, which does not discriminate between gamma-producing channels. CGMF simulations were used for evaluating the PFG multiplicity probability distribution, now included in the ENDF/B-VIII.0 evaluation using a recently approved ENDF-6 format.

Where available, we have used experimental data to guide the evaluation, or simulation results in the cases when modeling and experiment agree well with each other, as in the case of  $^{235}\text{U}(n,f)$  PFGs. The CGMF simulations tend to agree the best with data at thermal incident neutrons, even if not always in great detail. However, for fast neutrons, the discrepancy between CGMF and the

TABLE III. The same as in Table I, but for the  $^{239}\text{Pu}(n_{\text{th}},f)$  reaction.

	$E_{\text{thresh}}$	$\langle M_{\gamma} \rangle$	$\langle \varepsilon_{\gamma} \rangle$	$\langle E_{\gamma}^{\text{tot}} \rangle$
ENDF/B-VIII.0	0	7.56	0.84	6.37
ENDF/B-VII.1		7.78	0.87	6.74
JEFF 3.3		7.89	0.80	6.34
JENDL 4		8.34	0.89	7.45
ENDF/B-VIII.0	0.10	7.33	0.87	6.35
ENDF/B-VII.1	0.10	7.38	0.91	6.72
Pleasanton [60]	0.09	6.88(35)	0.98(7)	6.73(35)
Gatera [57]	0.10	7.35(12)	0.85(2)	6.27(11)
CGMF	0.10	7.57	0.87	6.71
ENDF/B-VIII.0	0.14	7.07	0.89	6.32
ENDF/B-VII.1	0.14	7.14	0.94	6.69
Verbinski [35]	0.14	7.23(30)	0.94(5)	6.81
CGMF	0.14	7.12	0.94	6.66
Ullmann [44]	0.15	7.15(9)		7.46(6)
Chyzh [36]	0.15	7.93		6.94

newest evaluation increases with increasing the incident energy, for both the average PFG multiplicity and average total gamma-ray energy released. At the moment, most of the fine tuning in CGMF is done at thermal incident energy, where more experimental data are available. For higher incident energies more parameters will have to be readjusted to provide better agreement with the data. However, at least in the case of the  $^{235}\text{U}(n,f)$  reaction, the Fréhaut CEA data [46] for the average total gamma-ray energy is much closer to CGMF results and shows a large discrepancy with the current evaluation, which was informed by the Drake data on total gamma production cross section. But because these data points are not well documented in terms of time coincidence window, or energy detection threshold, it is difficult to draw a definitive conclusion. New measurements of the PFG properties as a function of incident neutron energy would be very helpful for an update of the current evaluation. One should also emphasize our use of data not published in peer-reviewed journals, even though measurements have been performed. In order to compare with the current evaluation, we have been forced in quite a few cases to use data digitized from available conference proceedings.

The method to extract the average multiplicity from the total gamma cross section works well in the cases where fission dominates. However, when this is not the case (see Sec. III B on  $^{238}\text{U}$  evaluation), we observe a large discrepancy between the evaluation and data. This can be due to the improper treatment of the other gamma production channels, like in the top left panel of Fig. 13 for  $^{238}\text{U}$ , where the capture gamma production that dominates at 1.09 MeV incident energy clearly has a different shape than the experimental data. However, new experimental data with fast neutrons are necessary in order to provide better constraints on the evaluation.

At the moment, the ENDF-6 format does not allow us to record any information about timing, although from both simulations and experimental results, PFG proper-

ties depend more or less strongly on the time from fission, due to the existence of the long-lived (isomeric) excited states in fission fragments. In CGMF calculations, the value of average PFG multiplicity can increase by up to about 8% when the time coincidence window varies from a few nanoseconds to a few minutes [6, 45]. For the same quantity, FREYA predicts a weaker, although still significant, dependence of the time since fission, see Fig. 45 in Ref. [6]. In the current evaluation, all the simulations have been performed with a 6 ns coincidence window. Future formats will have to be accepted in order to provide PFG data that can be used in a number of applications, where the coincidence window can be significantly longer than it is currently (implicitly) set in the present evaluation.

## ACKNOWLEDGEMENTS

We thank A. Tudora for providing the PFG data shown in Fig. 11, and to A. Oberstedt for their gamma evaluation data for all three reactions included in this paper.

The work of I.S., M.B.C., P.T. and T.K. was performed at Los Alamos National Laboratory, under the auspices of the National Nuclear Security Administration of the U.S. Department of Energy. This material is based upon work partially supported by the Department of Energy Nuclear Criticality Safety Program, funded and managed by the National Nuclear Security Administration for the U.S. Department of Energy.

- 
- [1] D. Brown, M. Chadwick, R. Capote *et al.*, “ENDF/B-VIII.0: The 8th major release of the nuclear reaction data library with CIELO-project cross sections, new standards and thermal scattering data,” *NUCL. DATA SHEETS* **148**, 1 (2018). Special Issue on Nuclear Reaction Data.
- [2] M. Chadwick, M. Herman, P. Obložinský *et al.*, “ENDF/B-VII.1 nuclear data for science and technology: Cross sections, covariances, fission product yields and decay data,” *NUCL. DATA SHEETS* **112**, 2887 (2011). Special Issue on ENDF/B-VII.1 Library.
- [3] P. Talou, T. Kawano, and I. Stetcu, “CGMF documentation,” Tech. Rep. LA-UR-14-24031, Los Alamos National Laboratory (2014).
- [4] J. Verbeke, J. Randrup, and R. Vogt, “Fission reaction event yield algorithm FREYA 2.0.2,” *COMPUT. PHYS. COMMUN.* **222**, 263 (2018).
- [5] C. J. Werner, J. S. Bull, C. J. Solomon *et al.*, “MCNP Version 6.2. release notes,” Tech. Rep. LA-UR-18-20808, Los Alamos National Laboratory (2018).
- [6] P. Talou, R. Vogt, J. Randrup *et al.*, “Correlated prompt fission data in transport simulations,” *EUR. PHYS. J. A* **54**, 9 (2018).
- [7] R. Capote, D. L. Smith, and A. Trkov, “Nuclear data evaluation methodology including estimates of covariances,” *EPJ WEB CONF.* **8**, 04001 (2010).
- [8] A. C. Wahl, “Systematics of fission-product yields,” Report LA-13928, Los Alamos National Laboratory (2002).
- [9] B. Becker, P. Talou, T. Kawano, Y. Danon, and I. Stetcu, “Monte Carlo Hauser-Feshbach predictions of prompt fission  $\gamma$  rays: Application to  $n_{th} + {}^{235}\text{U}$ ,  $n_{th} + {}^{239}\text{Pu}$ , and  ${}^{252}\text{Cf}$  (sf),” *PHYS. REV. C* **87**, 014617 (2013).
- [10] I. Stetcu, P. Talou, T. Kawano, and M. Jandel, “Properties of prompt-fission  $\gamma$  rays,” *PHYS. REV. C* **90**, 024617 (2014).
- [11] I. Stetcu, P. Talou, and T. Kawano, “Neutron-induced fission: properties of prompt neutron and  $\gamma$  rays as a function of incident energy,” *EPJ WEB CONF.* **122**, 01012 (2016).
- [12] I. Stetcu, P. Talou, and T. Kawano, “Prompt fission neutron and  $\gamma$ -ray properties as a function of incident neutron energy,” *EPJ WEB CONF.* **146**, 04026 (2017).
- [13] A. Oberstedt, P. Halipré, F. J. Hambsch, M. Lebois, S. Oberstedt, and J. N. Wilson, “Prompt fission  $\gamma$ -ray spectra characteristics – systematics and predictions,” *PHYS. PROCEDIA* **64**, 91 (2015).
- [14] A. Oberstedt, R. Billnert, and S. Oberstedt, “Predictions of characteristics of prompt-fission  $\gamma$ -ray spectra from the  $n + {}^{238}\text{U}$  reaction up to  $E_n = 20\text{ MeV}$ ,” *PHYS. REV. C* **96**, 034612 (2017).
- [15] H. Nifenecker, C. Signarbieux, M. Ribrag, J. Poitou, and J. Matuszek, “Gamma-neutron competition in the de-excitation mechanism of the fission fragments of  ${}^{252}\text{Cf}$ ,” *NUCL. PHYS. A* **189**, 285 (1972).
- [16] P. Glässel, R. Schmid-Fabian, D. Schwalm, D. Habs, and H. Helmolt, “ ${}^{252}\text{Cf}$  fission revisited — new insights into the fission process,” *NUCL. PHYS. A* **502**, 315 (1989).
- [17] D. Bleuel, L. Bernstein, J. Burke *et al.*, “Gamma-ray multiplicity measurement of the spontaneous fission of  ${}^{252}\text{Cf}$  in a segmented HPGe/BGO detector array,” *NUCL. INSTR. METH. PHYS. RES. A* **624**, 691 (2010).
- [18] T. Wang, G. Li, L. Zhu *et al.*, “Correlations of neutron multiplicity and  $\gamma$ -ray multiplicity with fragment mass and total kinetic energy in spontaneous fission of  ${}^{252}\text{Cf}$ ,” *PHYS. REV. C* **93**, 014606 (2016).
- [19] M. J. Marcatch, R. C. Haight, R. Vogt, M. Devlin, P. Talou, I. Stetcu, J. Randrup, P. F. Schuster, S. D. Clarke, and S. A. Pozzi, “Measured and simulated  ${}^{252}\text{Cf}$ (sf) prompt neutron-photon competition,” *PHYS. REV. C* **97**, 044622 (2018).
- [20] A. Tudora, private communication (2018).
- [21] A. Tudora, B. Morillon, F.-J. Hambsch, G. Vladuca, and S. Oberstedt, “A refined model for  ${}^{235}\text{U}$ (n,f) prompt fission neutron multiplicity and spectrum calculation with validation in integral benchmarks,” *NUCL. PHYS. A* **756**, 176 (2005).
- [22] D. G. Madland and J. R. Nix, “New calculation of prompt fission neutron spectra and average prompt neutron multiplicities,” *NUCL. SCI. ENG.* **81**, 213 (1982).
- [23] E. Kwan, C. Wu, R. Haight *et al.*, “Prompt energy distribution of  ${}^{235}\text{U}$ (n,f) $\gamma$  at bombarding energies of 1–20 MeV,” *NUCL. INSTR. METH. PHYS. RES. A* **688**, 55 (2012).
- [24] J.-M. Laborie, G. Belier, and J. Taieb, “Measurement of prompt fission  $\gamma$ -ray spectra in fast neutron-induced fission,” *PHYS. PROCEDIA* **31**, 13 (2012). GAMMA-1 Emission of Prompt Gamma-Rays in Fission and Related Topics.
- [25] D. O. Nellis and I. L. Morgan, “Gamma-ray production

- cross sections for U235, U238, and Pu239,” Tech. Rep. 2791, Oak Ridge National Laboratory (1966).
- [26] D. M. Drake, “Inelastic neutron scattering and gamma production from fast-neutron bombardment of  $^{235}\text{U}$ ,” NUCL. PHYS. A **133**, 108 (1969).
- [27] D. M. Drake, J. C. Hopkins, C. S. Young, and H. Condé, “Gamma-ray-production cross sections for fast neutron interactions with several elements,” NUCL. SCI. ENG. **40**, 294 (1970).
- [28] D. M. Drake, “Cross sections of Uranium-235 and Plutonium-239 for neutrons producing gamma rays,” NUCL. SCI. ENG. **55**, 427 (1974).
- [29] D. M. Drake, E. D. Arthur, and M. G. Silbert, “Cross Sections for Gamma-Ray Production by 14-MeV Neutrons,” NUCL. SCI. ENG. **65**, 49 (1978).
- [30] L. Steward and R. E. Hunter, “Evaluated neutron-induced gamma-ray production cross sections for  $^{235}\text{U}$  and  $^{238}\text{U}$ ,” Los Alamos National Laboratory Report No. LA-4918 (1972).
- [31] F. Pleasonton, R. L. Ferguson, and H. W. Schmitt, “Prompt gamma rays emitted in the thermal-neutron-induced fission of  $^{235}\text{U}$ ,” PHYS. REV. C **6**, 1023 (1972).
- [32] A. Oberstedt, T. Belgia, R. Billnert *et al.*, “Improved values for the characteristics of prompt-fission  $\gamma$ -ray spectra from the reaction  $^{235}\text{U}(n_{\text{th}}, f)$ ,” PHYS. REV. C **87**, 051602 (2013).
- [33] A. Oberstedt, private communication (2017).
- [34] S. Oberstedt, private communication (2017).
- [35] V. V. Verbinski, H. Weber, and R. E. Sund, “Prompt gamma rays from  $^{235}\text{U}(n, f)$ ,  $^{239}\text{Pu}(n, f)$ , and spontaneous fission of  $^{252}\text{Cf}$ ,” PHYS. REV. C **7**, 1173 (1973).
- [36] A. Chyzh, C. Y. Wu, E. Kwan, R. A. Henderson, T. A. Bredeweg, R. C. Haight, A. C. Hayes-Sterbenz, H. Y. Lee, J. M. O’Donnell, and J. L. Ullmann, “Total prompt  $\gamma$ -ray emission in fission of  $^{235}\text{U}$ ,  $^{239,241}\text{Pu}$ , and  $^{252}\text{Cf}$ ,” PHYS. REV. C **90**, 014602 (2014).
- [37] R. W. Peelle and F. C. Maienschein, “Spectrum of photons emitted in coincidence with fission of  $^{235}\text{U}$  by thermal neutrons,” PHYS. REV. C **3**, 373 (1971).
- [38] M. Jandel, T. A. Bredeweg, E. M. Bond *et al.*, “Prompt  $\gamma$ -ray emission in neutron induced fission of  $^{235}\text{U}$ ,” Tech. Rep. LA-UR-12-24975, Los Alamos National Laboratory (2013), to be published.
- [39] T. Valentine, “Evaluation of prompt fission gamma rays for use in simulating nuclear safeguard measurements,” Tech. Rep. ORNL/TM-1999/300, Oak Ridge National Laboratory (1999).
- [40] T. E. Valentine, “Evaluation of prompt fission gamma rays for use in simulating nuclear safeguard measurements,” ANN. NUCL. ENG. **28**, 191 (2001).
- [41] A. Chyzh, C. Y. Wu, E. Kwan *et al.*, “Systematics of prompt  $\gamma$ -ray emission in fission,” PHYS. REV. C **87**, 034620 (2013).
- [42] K. Nishio, private communication (2016).
- [43] V. M. Gorbachev, V. I. Nagornyy, Y. Y. Nefedov, M. S. Shvetsov, E. F. Fomushkin, and A. M. Shvetsov, “Gamma-ray production cross-section for interactions of 13.8 MeV neutrons with Cu, W and U-235 nuclei,” in *Conf. on Nucl. Data for Sci. and Techn.*, **2**, 950 (1994).
- [44] J. L. Ullmann, E. M. Bond, T. A. Bredeweg *et al.*, “Prompt  $\gamma$ -ray production in neutron-induced fission of  $^{239}\text{Pu}$ ,” PHYS. REV. C **87**, 044607 (2013).
- [45] P. Talou, T. Kawano, I. Stetcu, J. P. Lestone, E. McKeigney, and M. B. Chadwick, “Late-time emission of prompt fission  $\gamma$  rays,” PHYS. REV. C **94**, 064613 (2016).
- [46] J. Fréhaut, A. Bertin, and R. Bois, “Mesure de  $\bar{\nu}_p$  pour la fission de  $^{232}\text{Th}$ ,  $^{235}\text{U}$  et  $^{237}\text{Np}$  induite par des neutrons d’énergie comprise entre 1 et 15 MeV,” in *International Conference on Nuclear Data for Science and Technology, Antwerp, Belgium*, 78, Reidel, Dordrech, Holland (1983).
- [47] D. G. Madland, “Total prompt energy release in the neutron-induced fission of  $^{235}\text{U}$ ,  $^{238}\text{U}$ , and  $^{239}\text{Pu}$ ,” NUCL. PHYS. A **772**, 113 (2006).
- [48] M. Lebois, J. N. Wilson, P. Halipré *et al.*, “Comparative measurement of prompt fission  $\gamma$ -ray emission from fast-neutron-induced fission of  $^{235}\text{U}$  and  $^{238}\text{U}$ ,” PHYS. REV. C **92**, 034618 (2015).
- [49] L. Qi, M. Lebois, J. N. Wilson *et al.*, “Statistical study of the prompt-fission  $\gamma$ -ray spectrum for  $^{238}\text{U}(n, f)$  in the fast-neutron region,” PHYS. REV. C **98**, 014612 (2018).
- [50] O. Serot, “Prompt fission gamma spectra and multiplicities for JEFF-3.3,” Tech. Rep. JEFF/DOC-1828, OECD NEA (2017).
- [51] A. Tudora, G. Vladuca, and B. Morillon, “Prompt fission neutron multiplicity and spectrum model for 30–80 MeV neutrons incident on  $^{238}\text{U}$ ,” NUCL. PHYS. A **740**, 33 (2004).
- [52] A. Tudora, F.-J. Hamsch, and S. Oberstedt, “Sub-barrier resonance fission and its effects on fission fragment properties,” NUCL. PHYS. A **890-891**, 77 (2012).
- [53] A. A. Filatenkov, M. V. Blinov, S. V. Chuvaev, and V. M. Saidgareev, “Cross-sections for the production of gamma-ray by the interaction of 3.0 MeV neutrons with Th-232, U-235, U-238 nuclei,” VOP. AT. NAUKI I TEKH., SER. YADERNYE KONSTANTY **2**, 56 (1988).
- [54] Y. Y. Nefedov, V. I. Nagornyy, V. I. Semenov, A. K. Zhitnik, R. A. Orlov, and A. E. Shmarov, “Gamma-ray production cross-section and spectrum measurement results for inelastic interaction of 14 MeV neutrons with nuclei of Na, S, Cl, Ti, V, Cr, Ni, Zn, Ge, Nb, Cd, In, Sn, Bi,  $^{235}\text{U}$  and  $^{238}\text{U}$ ,” VOP. AT. NAUKI I TEKH., SER. YADERNYE KONSTANTY **1**, 7 (2000).
- [55] R. Capote, A. Trkov, M. Sin *et al.*, “IAEA CIELO evaluation of neutron-induced reactions on  $^{235}\text{U}$  and  $^{238}\text{U}$  targets,” NUCL. DATA SHEETS **148**, 254 (2018). Special Issue on Nuclear Reaction Data.
- [56] A. Carlson, V. Pronyaev, R. Capote *et al.*, “Evaluation of the neutron data standards,” NUCL. DATA SHEETS **148**, 143 (2018). Special Issue on Nuclear Reaction Data.
- [57] A. Gatera, T. Belgia, W. Geerts *et al.*, “Prompt-fission  $\gamma$ -ray spectral characteristics from  $^{239}\text{Pu}(n_{\text{th}}, f)$ ,” PHYS. REV. C **95**, 064609 (2017).
- [58] D. Choudhury, A. Gatera, A. Göök, M. Lebois, A. Oberstedt, S. Oberstedt, L. Qi, and J. Wilson, “High-precision prompt fission gamma-ray studies for nuclear reactor safety,” J. NUCL. RES. DEV. **14**, 16 (2017).
- [59] E. Fort, J. Fréhaut, and P. Long, “Prompt gammas emitted in fission,” Tech. Rep. JEFF/DOC-219, OECD NEA (1988).
- [60] F. Pleasonton, “Prompt  $\gamma$ -rays emitted in the thermal-neutron induced fission of  $^{233}\text{U}$  and  $^{239}\text{Pu}$ ,” NUCL. PHYS. A **213**, 413 (1973).